AGU PUBLICATIONS

Tectonics

RESEARCH ARTICLE
10.1002/2016TC004414

Special Section:
Orogenic cycles: from field observations to global geodynamics

An evaporite-bearing accretionary complex in the northern front of the Betic-Rif orogen

Fernando Pérez-Valera[1,2], Mario Sánchez-Gómez[1,3], Alberto Pérez-López[4,5], and Luis Alfonso Pérez-Valera[1]

[1]Centro de Estudios Avanzados en Ciencias de la Tierra (Universidad de Jaén), Jaén, Spain, [2]Departamento de Ciencias de la Tierra y del Medio Ambiente, Universidad de Alicante, Alicante, Spain, [3]Departamento de Geología, Facultad de Ciencias Experimentales (Universidad de Jaén), Jaén, Spain, [4]Departamento de Estratigrafía y Paleontología, Facultad de Ciencias (Universidad de Granada), Granada, Spain, [5]Instituto Andaluz de Ciencias de la Tierra (CSIC-Universidad de Granada), Armilla, Spain

Abstract The Guadalquivir Accretionary Complex forms a largely oblique prism at the northern edge of the Betic-Rif orogen, where Miocene sediments plus allochthonous evaporite-bearing units were accreted during the displacement of the Alborán Domain toward the west. Traditional interpretations end the tectonic structuring of the Betic Cordillera at the present topographic front, beyond which gravitational and/or diapiric processes would predominate. However, this study shows pervasive tectonic deformation in the outer prism with coherent oblique shortening kinematics, which is achieved through an alternation of roughly N-S arcuate thrust systems connected by E-W transfer fault zones. These structures accord well with the geophysical models that propose westward rollback subduction. The main stage of tectonic activity occurred in the early-middle Miocene, but deformation lasted until the Quaternary with the same kinematics. Evaporite rocks played a leading role in the deformation as evidenced by the suite of ductile structures in gypsum distributed throughout the area. S- and L- gypsum tectonites, scaly clay fabrics, and brittle fabrics coexist and consistently indicate westward motion (top to 290°), with subordinate N-S contraction almost perpendicular to the transfer zones. This work reveals ductile tectonic fabrics in gypsum as a valuable tool to elucidate the structure and deformational history of complex tectonic mélanges involving evaporites above the décollement level of accretionary wedges.

Key Points:
- Evaporite-bearing units form an accretional complex in Betics north end
- Evaporites display a suite of ductile structures with coherent kinematics
- Kinematics indicate westward motion, with subordinate N-S contraction

Correspondence to:
F. Pérez-Valera,
fperez@ujaen.es

Citation:
Pérez-Valera, F., M. Sánchez-Gómez, A. Pérez-López, and L. A. Pérez-Valera (2017), An evaporite-bearing accretionary complex in the northern front of the Betic-Rif orogen, *Tectonics*, *36*, 1006–1036, doi:10.1002/2016TC004414.

Received 8 NOV 2016
Accepted 24 APR 2017
Accepted article online 21 MAY 2017
Published online 1 JUN 2017

1. Introduction

Highly arcuate orogens throughout the Earth have puzzled researchers regarding the involved lithosphere mechanisms [e.g., *Ghiglione and Cristallini*, 2007; *Copley*, 2012; *Boutelier and Cruden*, 2013; *Sippl et al*., 2013; *Moresi et al*., 2014; *Hodges and Miller*, 2015] and mode of deformation and strain partitioning in the upper crust [*Egydio-Silva et al*., 2005; *Murphy and Copeland*, 2005; *Del Ben et al*., 2008; *Rosenbaum*, 2012; *Shaw et al*., 2016]. The Betic-Rif orogen configure an extremely tight orogenic arc, namely, the Gibraltar Arc, superimposed to a converging Africa and Iberia plate boundary [*Platt et al*., 2003].

In the past two decades, a number of authors has proposed that the lithospheric process responsible for the formation of the Gibraltar Arc is a subduction zone rollback [*Lonergan and White*, 1997], involving both oceanic and continental lithospheric mantle slab retreat [*Duggen et al*., 2004, 2005], which, in turn, has been confirmed by recent geophysical studies [*Bokelmann et al*., 2011; *Rosell et al*., 2011; *Gutscher et al*., 2012; *Bezada et al*., 2013; *Mancilla et al*., 2015]. This mechanism, as originally formulated by *Lonergan and White* [1997], could explain the coeval shortening and extension structures largely observed and discussed in the Alboran Domain or internal zone of the Betics and Rif [e.g., *Martínez-Martínez and Azañón*, 1997; *Balanyá et al*., 1998; *Martínez-Martínez et al*., 2002; *Giaconia et al*., 2014; *Galindo-Zaldivar et al*., 2015]. Furthermore, the combination of tearing caused by rollback and shortening caused by continuing plate convergence must have given way to oblique convergence, especially at the edges of the Betic-Rif orocline [*Lonergan and White*, 1997], namely, at the outermost deformed foreland paleomargins. Actually, structures that could accommodate the oblique convergence as large transpressive fault zones are well known in the Alborán Domain [*Martínez-Martínez*, 2006; *Barcos et al*., 2015] or in the Rif [*Leblanc*, 1990; *Vitale et al*., 2015], but not in the thin-skinned fold-and-thrust belt of the external Betics (the Subbetic and Prebetic units), where only one of these structures has been described, the so-called Socovos Fault [*Pérez-Valera et al*., 2013].

Up to now, large sectors of the external Betic fold-and-thrust belt and their contact with the foreland basin (Guadalquivir Basin) remain relatively unknown from a structural point of view and without a tangible connection with the current orogenic models. In this way, it is assumed that large structures are absent or obliterated by a wide "chaotic belt" composed by heterogeneous blocks embedded in a brecciated gypsum-rich matrix that have been formally interpreted as a gravitational olistostromic unit [*Roldán-García et al*., 2012; *Ruiz-Constán et al*., 2012; *Rodríguez-Fernández et al*., 2013]. Nevertheless, the apparent "chaotic" aspect of the outcropping rocks and the lack of mapped structures have not been an obstacle to propose contradictory tectonic models in this area [*Pedrera et al*., 2013; *Morales et al*., 2015] to explain recent seismicity [*Serrano et al*., 2015].

The so-called chaotic units are common elements of accretionary wedges in the frontal part of fold-and-thrust belts worldwide [*Kulm and Suess*, 1990; *Burg et al*., 2008; *Codegone et al*., 2012]. In these contexts, fragmented rock units with predominance of stratal disruption and/or mixing processes resulting in a wide variety of rocks with multiple genetic associations (sedimentary, tectonic, diapiric, or combination of these) are still controversial issues [*Cowan*, 1985; *Harris et al*., 1998; *Festa et al*., 2010, 2015; *Vannucchi and Bettelli*, 2010; *Pini et al*., 2012]. Moreover, most of the present and past accretionary wedges with chaotic complexes involve pelagic detrital sediments from deep basins [*Westbrook et al*., 1988; *Moore et al*., 1990; *Schlüter et al*., 2002; *Lucente and Pini*, 2008], but a scarce number of them show evaporitic rocks since evaporites usually act as preferred detachment levels [e.g., *Davis and Engelder*, 1985; *Costa and Vendeville*, 2002; *Krzywiec and Vergés*, 2007]. Therefore, the abundance of evaporite-bearing units in the most external units of the Betic Cordillera constitutes an unusual case of orogenic wedge, which controls the structural style [e.g., *Luján et al*., 2000, 2003; *Crespo-Blanc*, 2007].

The presence of highly plastic evaporitic rocks (mainly salt and gypsum) eases deformation in the form of ductile structures such as folds, foliations, and lineations, suitable of being analyzed geometrically, in particular into salt [*Schorn et al*., 2013a] and also into gypsum [*Malavieille and Ritz*, 1989; *De Paola et al*., 2008; *Schorn and Neubauer*, 2011; *Schorn et al*., 2013b]. In this paper, we study a sector of the central Betic Cordillera formed by evaporite-bearing units in contact with the Guadalquivir foreland basin and connecting the two main arcs (Cazorla and Gibraltar) in the north branch of the orogen [*Balanyá et al*., 2007] that is affected by a transpression-dominated tectonic regime.

We evaluate the kinematics and geometry of the structures based on field and geophysical data. In particular, gypsum fabrics show their potential to establish the tectonic pattern in this complex geological context. The identification and analysis of kinematic indicators is relevant to elucidate the genetic processes that have been proposed, including diapiric [*Berástegui et al*., 1998] or tectonic (accretionary wedge)-driven mechanisms [*Flinch*, 1996], besides the hypothesis of the gravitational chaotic complex. Our work reveals a previously hidden organization that is compared with those predicted by the current orogenic hypothesis to explain the extremely arcuate shape of the Betic-Rif orogen.

2. Geological Setting

The Betic and Rif Cordilleras form the so-called Gibraltar Arc and constitute the westernmost termination of the Alpine Mediterranean belt. The Gibraltar Arc is a very tight arcuate structure formed during the Miocene [*Andrieux et al*., 1971; *Platt et al*., 1995; *Luján et al*., 2003; *Platt et al*., 2003; *Balanyá et al*., 2007] as the result of the westward emplacement of a metamorphic terrain named the Alboran Domain (Betic-Rif Internal Zones) [e.g., *Balanyá and García-Dueñas*, 1987; *Martínez-Martínez and Azañón*, 1997] over the South Iberian and Maghrebian paleomargins. Few geodynamic models have been proposed to explain the mechanisms driving this process. The first tectonics models proposed for the Gibraltar Arc involved the collapse of a thickened lithosphere [e.g., *Platt and Vissers*, 1989; *Platt et al*., 2003] or mantle delamination after continental oblique collision [e.g., *García-Dueñas et al*., 1992; *Docherty and Banda*, 1995; *Seber et al*., 1996; *Calvert et al*., 2000; *Fadil et al*., 2006]. On the contrary, the most recent hypotheses propose oceanic subduction associated with slab rollback [e.g., *Lonergan and White*, 1997; *Durand-Delga et al*., 2000; *Faccenna et al*., 2004; *Spakman and Wortel*, 2004; *Michard et al*., 2005; *Duggen et al*., 2008; *Bokelmann et al*., 2011; *García-Castellanos and Villaseñor*, 2011]. In all of these tectonic models, the collision of the Alborán Domain results in detachment of the Mesozoic sedimentary cover from the Iberian and Maghrebian paleomargins, which, in turn, imbricate and arrange into two fold-and-thrust belts, namely, the Betic and Rif External Zones [*Flinch*, 1996;

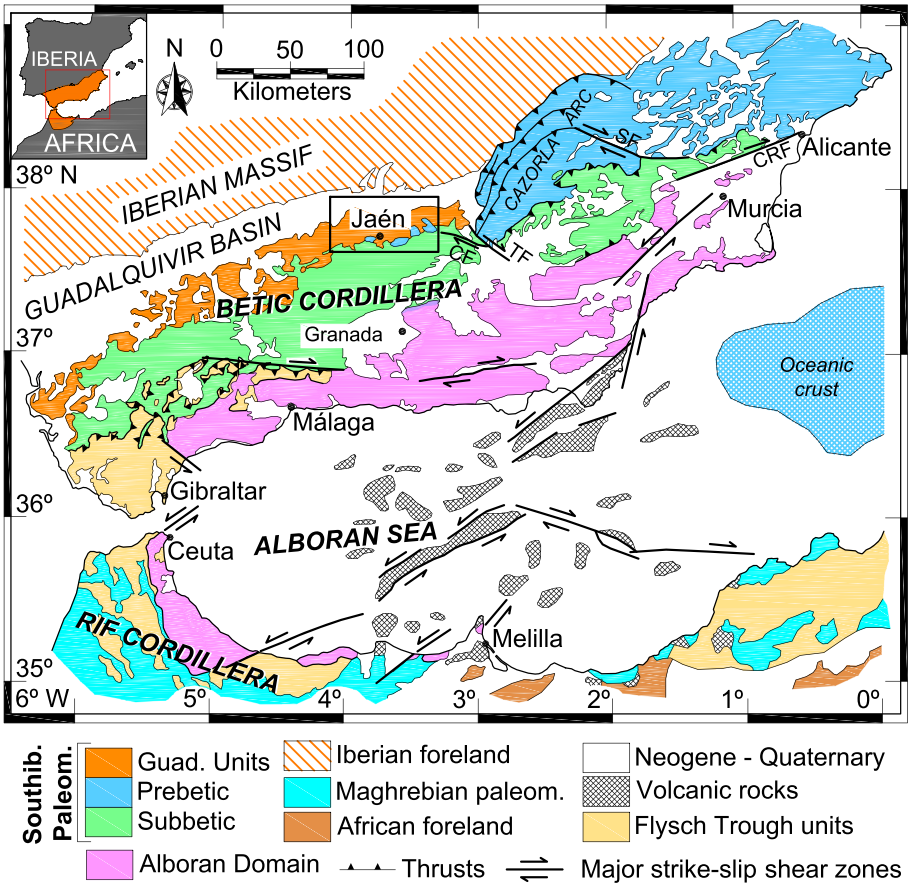

Figure 1. Geological map of the Betic-Rif orogen, modified from *Comas et al.* [1999], showing the regional study area in Figure 2. Map also shows major strike-slip faults and shear zones. Guad. Units: Guadalquivir Units. CRF: Crevillente Fault. SF: Socovos Fault. TF: Tíscar Fault. CF: Collejares Fault.

Crespo-Blanc and Campos, 2001]. The décollement level in the External Zones of the Betics is a Triassic sequence with clays and evaporites with hundred-meter thick layers of salt and Ca sulfates (gypsum and anhydrite) that originally reached thicknesses of up to or over 1000 m [*Pérez-López*, 1998]. In the eastern Betics, the fold-and-thrust belt ends directly against the Iberian Massif (Figure 1) and its very thin Mesozoic cover, which remains undeformed (Tabular Cover). In contrast, in the central and western Betics, the External Zones bound the Guadalquivir Basin, a foreland basin [*García-Castellanos*, 2002] with marine sedimentation from the middle Miocene to the Pliocene-Quaternary [*Fernàndez et al.*, 1998; *García-Castellanos et al.*, 2002]. The focus of this paper is on this boundary between the External Zones and the Guadalquivir Basin.

2.1. The Betic External Zones

The External Zones are a belt of allochthonous and parautochthonous units from the South Iberian paleomargin that are affected by thin-skinned tectonics in the Oligocene-Miocene [e.g., *Hermes*, 1985]. This belt is completely nonmetamorphic in contrast to the Alborán Domain, where three tectonic complexes have a pre-Miocene and Miocene polyphasic metamorphic history [*Balanyá et al.*, 1997; *Booth-Rea et al.*, 2005].

The External Zones are traditionally subdivided into a set of units based on their relative paleogeographic position with respect to the foreland, considering the stratigraphy of Jurassic and Cretaceous units. From proximal to distal areas, two main zones can be defined: (1) the Prebetic Zone, located in proximal areas, and (2) the Subbetic Zone, in a distal position [*García-Hernández et al.*, 1980; *Vera*, 2001]. The Prebetic Zone records sediments deposited in a nearshore, epicontinental platform during the Jurassic and Cretaceous. In contrast, the Subbetic Zone is composed of pelagic and hemipelagic rocks deposited in external, distal platform to basinal environments with thick successions of pelagic marls and marly limestones, reaching the

early Eocene in most sectors [*Vera and Molina*, 1999]. Starting in the late Oligocene-Miocene, with the beginning of the collision with the Alborán Domain, sedimentation over the External Zones became more discontinuous, resulting in the formation of progressively shallower and more isolated compartmented basins [*Rodríguez-Fernández and Sanz de Galdeano*, 1992; *Meijninger and Vissers*, 2007].

Beneath the Jurassic and Cretaceous units in the Prebetic and Subbetic zones, Triassic deposits are conspicuous in the Betic External Zones, constituting the so-called South Iberian Triassic [*Pérez-López*, 1998]. The South Iberian Triassic consists, from bottom to top, of (1) 100 m of epicontinental carbonates (Muschelkalk facies) [*Pérez-Valera and Pérez-López*, 2007]; (2) 400 to 500 m of multicolored shales, sandstones, gypsum, anhydrite, and salt (Keuper facies) [*Pérez-López*, 1996]; and (3) 40 m of thin carbonates (Zamoranos Formation) [*Pérez-López et al*., 2012] with a thick evaporitic sequence at the top (supra-Keuper). Nevertheless, the thickness of the whole Triassic series dramatically decreases toward the Prebetic from approximately 1000 m to 200 m, where carbonates and salt-bearing evaporites are replaced by more detrital sediments with subordinate layers of gypsum at the top [*Fernández and Dabrio*, 1985].

In the eastern Betics, the tectonic units that form each zone thrust to the northwest over the next most external one, forming a NNE-SSW orogenic arc [*Nebbad*, 2001] termed the Cazorla Arc (Figure 1). The Cazorla Arc is bounded to the north and south by strike-slip fault zones, both operating as dextral transfer faults of the west directed Betic displacements [*Guezou et al*., 1991; *Andrieux and Nebbad*, 1996; *Platt et al*., 2003]. In the south branch of the Cazorla Arc, the Tíscar Fault [*Frizon De Lamotte et al*., 1991; *Sanz de Galdeano et al*., 2006] and the Collejares Fault Zone [*Pérez-Valera et al*., 2012], with an average strike of 150° and 100°, respectively, transferred the displacement of the Subbetic units that overthrust the Prebetic front and are emplaced directly over the Guadalquivir Basin (Figure 1). The transport sense of the Subbetic tectonic units is varied, ranging from 000° and even 020° [*Guezou et al*., 1991] to 250° [*Ruano et al*., 2004]. The apparent lack of coherence of the kinematic vectors has contributed to the chaotic-like aspect attributed to this region [e.g., *Pérez-López and Sanz de Galdeano*, 1994].

2.2. The Guadalquivir Basin

The Guadalquivir Basin is one of the youngest foreland basins of the Alpine-Mediterranean orogens, considering the age of their sedimentary infill [*Fernàndez et al*., 1998; *García-Castellanos et al*., 2002]. It is triangle shaped, open to the Atlantic Ocean with an elongated ENE-WSW axis (Figure 1). The Iberian Massif constitutes the foreland to the north, and the Betic Cordillera forms the active margin to the south. To the east, the Guadalquivir Basin is limited by the Prebetic Cazorla Arc, whose emplacement took place in the Late Tortonian, closing the so-called North Betic Strait, a marine gateway that connected the Atlantic and Mediterranean before the uplift of the Cazorla Arc [*Meijninger and Vissers*, 2007; *Martín et al*., 2009]. The Guadalquivir Basin is formed of late Miocene to Quaternary autochthonous, intrabasin-derived sediments, although in western sectors (Cádiz province), middle Miocene sediment has been reported from well logs [*Riaza and Martínez del Olmo*, 1996]. These nearshore to offshore sediments were deposited in a classic, asymmetric foreland basin, in which (1) the northern margin (passive margin) comprises shallow marine and deltaic systems developed on the forebulge (several tens of meters in thickness), (2) the central part corresponds to the foredeep with accumulations of nearshore to turbiditic sediments (hundreds of meters in thickness), and (3) the southern margin (active margin) has sediments deposited in tectonically, discontinuous, controlled basins, over the Betic Cordillera allochthonous units.

The contact between the External Zones and the Guadalquivir Basin is an apparently chaotic wide band (up to 20 km) (Figure 1), showing a complex tectonic structure with alternating Triassic and Cretaceous Subbetic units with Miocene sediments and other Subbetic lithologies in minor proportions. The structure is consistent with the Betic External Zones displacements [*Pérez-Valera et al*., 2011b; *Pedrera et al*., 2012]. Nevertheless, the most accepted hypothesis to explain the area's complexity was proposed by *Perconig* [1960], who considers that the presence of mega-elements emplaced by gravitational sliding is a general, extensive "olistostromic unit" formed by blocks of exotic lithologies (olistolites) from the Betic External Zones, resedimented in the middle Miocene inside a gypsum-rich matrix of marine origin [*Roldán-García and García-Cortés*, 1988; *Roldán-García et al*., 2012]. In fact, one of the most characteristic features of the area is the abundance of Triassic gypsum masses at the surface that, in depth, are accompanied by large volumes of salt (indicated by oil-well logs and seismic profiles) [*Lanaja*, 1987]. To explain the large volumes of Triassic salt and other evaporitic rocks, *Berástegui et al*. [1998] propose their emplacement as a lateral diapir that constitutes a

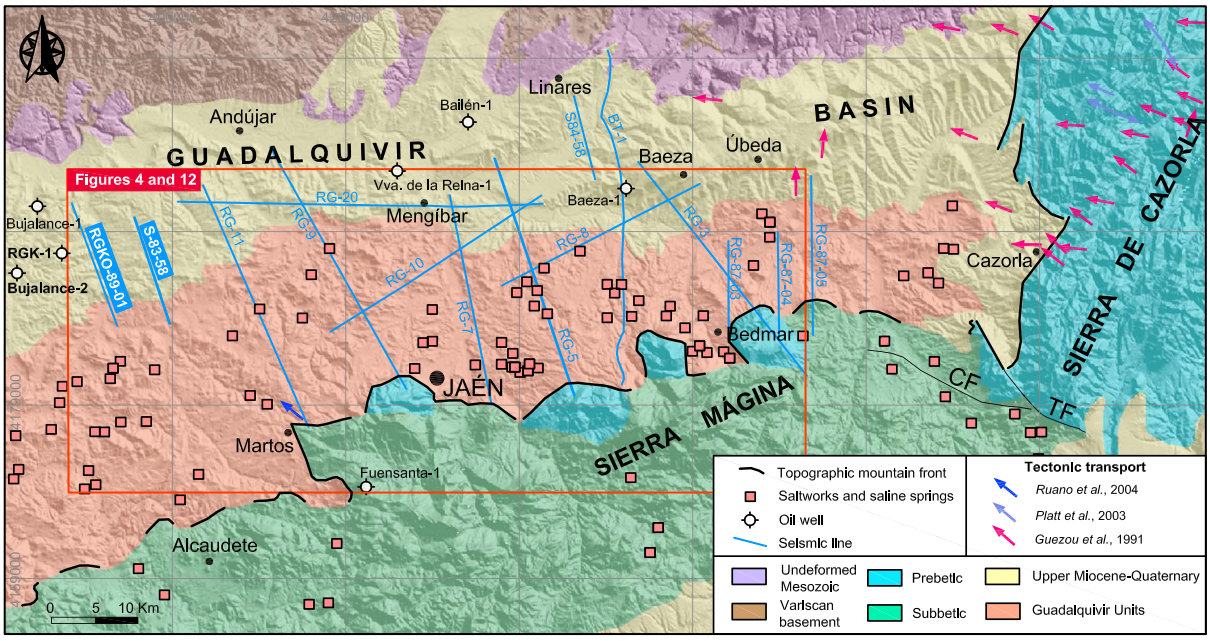

Figure 2. Geological simplified map (only major units) of the north end of the Betic orogen, showing the location of the main seismic lines (highlighted in blue), oil exploration wells, saltworks, and saline springs. Position of previous kinematic indicators is shown from *Guezou et al.* [1991], *Platt et al.* [2003], and *Ruano et al.* [2004]. TF: Tíscar Fault. CF: Collejares Fault.

"chaotic unit," together with frontal imbricate slices of Miocene sediments. On the other hand, it has been proposed that salt, after migration during the passive margin stage in the Late Cretaceous [*Flinch*, 2003], was emplaced as part of an accretionary wedge (Guadalquivir Allochthon [*Blankenship*, 1992; *Flinch et al.*, 1996]). However, none of the above hypotheses are supported by structural field data, and therefore, the olistostromic origin remains in the scientific literature as an explanation of the outcrop complexity, either as a cover that overlies deep, blind thrusts [e.g., *Ruano et al.*, 2004; *Motis and Martínez del Olmo*, 2012] or as a sedimentary mélange coexisting with a tectonic mélange [*Pedrera et al.*, 2012; *Rodríguez-Fernández et al.*, 2013].

The study area (Figures 1 and 2) comprises the northern front of the Betic Cordillera in contact with the southern margin of the eastern Guadalquivir Basin, where the Subbetic and Prebetic carbonate rocks outline an east-west mountain front almost parallel to the basin axis (Figure 2). North to this front, the basin is occupied by the set of allochthonous and chaotic-like units that we will call Guadalquivir Units (GUs), following the authors that recognized some grade of tectonic structuration (Figure 2), at least at local scales [*García-Rosell*, 1973; *Guezou et al.*, 1991; *Galindo-Zaldívar et al.*, 2000; *Platt et al.*, 2003; *Ruano et al.*, 2004].

3. Methodology

The data presented in this work derive mainly from a detailed field recognition and mapping of the northern portion of the Betic end in the Jaén area, in the southern Guadalquivir Basin. In order to support the structural interpretation in key zones with poor outcrop data, electrical tomography campaigns have been performed. In addition, several commercial reflection seismic lines carried out from 1982 to 1989 have been analyzed.

A key sector in the northernmost part of the study area, near Torrequebradilla town, has been mapped to the 1:40,000 scale to establish the structural style of the Torrequebradilla zone. In this sector, a deep, eroded stream (Arroyo Salado de Torrequebradilla) provides a unique and excellent natural transect, cutting approximately N-S across the western study area and exposing more than 8 km of distance of continuous outcrops.

Several representative outcrops with kinematic data are analyzed, selecting 31 structural measurement stations (Table 1). Cataclastic and ductile fabrics are penetrative and show clear kinematic criteria, well

Table 1. Detailed Structures and Kinematics of the Structural Stations

Station	Geographical Coordinates		Unit	Lithology[a]	Structures[b]	Kinematics
ALM-1	37.88284	−3.758777	Mélange type I	BR-GY	gf and gfb	Reverse
ANV-1	37.77106	−4.065698	Mélange type I	BR-GY	gf and gfb	Reverse
ANV-2	37.77244	−4.06733	Mélange type I	F-GY	gf	Reverse
ANV-3	37.77299	−4.066248	Capas Rojas Formation	SC-CL	cfl and sl	Reverse
ANV-4	37.77543	−4.07107	Capas Rojas Formation	SC-CL	cfl and sl	Reverse, strike slip
ARG-1	37.81942	−3.824776	Mélange type I	BR-GY	gf and gfb	Reverse
ARG-2	37.82027	−3.824683	Triassic (Keuper)	GY	gf and gfb	Reverse
ASN-1	37.81868	−3.724399	Mélange type I	BR-GY	gf, rml, and fa	Reverse
ASN-2	37.77866	−3.695369	Mélange type I	F-GY	gf, rml, and fa	Strike slip
ASN-3	37.8174	−3.722019	Mélange type I	F-GY	gf and rml	Strike slip
AST-1	37.88369	−3.667642	Mélange type I	F-GY	gf, rml, and fa	Reverse
AST-2	37.88876	−3.665754	Mélange type I	F-GY	gf and rml	Reverse
AST-3	37.8786	−3.662025	Mélange type I	BR-GY	gf and gfb	Reverse
AST-4	37.86646	−3.65456	Mélange type I	F-GY	gfb and rml	Strike slip
AST-5	37.89342	−3.67065	Mélange type I	BR-GY	gfb	Reverse
AST-6	37.90312	−3.725226	Mélange type I	F-GY	rml	Reverse
AST-7	37.91162	−3.674351	Mélange type II	SC-CL	cfl and sl	Reverse
ATY-1	37.86266	−3.422198	Mélange type I	F-GY	gf and rml	Strike slip
ATY-2	37.87204	−3.434656	Mélange type I	F-GY	gf	Strike slip
ATY-3	37.86254	−3.417616	Mélange type I	F-GY	gf, rml, and fa	Strike slip
CFR-1	37.87922	−3.895817	Mélange type II	F-GY	gf and fa	Strike slip
CFR-2	37.92137	−3.943931	Mélange type I	F-GY	gf and fa	Strike slip
CFR-3	37.91089	−3.931102	Mélange type I	F-GY	gf and rml	Strike slip
CFR-4	37.91721	−3.935835	Mélange type I	F-GY	gf, fa, and flt	Strike slip
GAR-1	37.87025	−3.462286	Mélange type I	F-GY	gf, rml, and fa	Reverse
GDB-1	37.81643	−3.748781	Mélange type I	F-GY	gf and rml	Reverse
HIG-1	37.8765	−3.886254	Lower Miocene	SC-CL	cfl and sl	Strike slip
SIB-1	37.92345	−3.612622	Mélange type I	F-GY	gf, rml, gfb, and flt	Reverse, strike slip
SMA-1	37.67921	−3.956394	Mélange type I	BR-GY	gf and gfb	Normal
SMA-2	37.67139	−3.994564	Upper Triassic	DOL	flt and sl	Strike slip
VDT-1	37.94704	−3.620037	Middle Miocene	SC-CL	cfl and sl	Reverse

[a]F-GY: foliated gypsum. BR-GY: brecciated gypsum. GY: gypsum. SC-CL: scaly clays, P-R composite fabrics; DOL: dolostones.
[b]gf: gypsum foliation. cfl: cataclastic foliation. Mineral lineations (rml: rods, mineral cluster, and mineral grain lineations; gfb: gypsum fibers in planes). fa: (sheath) fold axes. flt: discrete faults; sl: slickenlines (in discrete planes or distributed on P-R composite fabric).

preserved in gypsum-bearing rocks and/or lutites (clay-rich rocks), in which scaly fabric is also developed. Therefore, the kinematic data used consist of a wide set of linear features, ranging from pervasive slickenlines in clay-bearing rocks to mineral lineation (stretching lineation) in gypsum fabrics, including pressure shadows and gypsum tails over rigid clasts. Moreover, the direction (trend) of sheath fold axes has been used as kinematic data in shear zones with high strain values.

The electrical resistivity tomography method was undertaken with a dipole-dipole configuration. The dipole-dipole method uses two current electrodes on one side and two potential electrodes on the other side. The method is especially suitable for the detection of vertical structures as it penetrates to deeper levels [*Seaton and Burbey*, 2002; *Candansayar*, 2008]. Measuring was performed with electrodes spaced 5 m apart on the outcrop surface using an ABEM Terrameter SAS 1000 instrument. Data were processed through a 2-D inverse method using the EarthImager 2-D software, which images subsurface structures from electrical measurements made at the surface. Although the maximum depth of penetration was 60 m, this method is very interesting to locally compare the structure of stratified sedimentary layers at the subsurface.

A seismic line database is available from the Spanish Geological Survey (IGME) in the studied sector (see Figure 2). The quality of the seismic lines is generally poor, but two representative lines (Figure 2) have been chosen as demonstrative of different structural styles in deep. The seismic line interpretation has been supported by the data (lithology, age, and thickness) of nearby oil exploration wells [*Lanaja*, 1987].

4. Stratigraphy of the Guadalquivir Units

The term Guadalquivir Units (GUs) is used to define a set of allochthonous units present in the limit between the Betic Cordillera and the Guadalquivir Basin. These units show diverse stratigraphic and structural features that complicate their identification as individualized units differentiated in other areas of the Betic Cordillera. In the field, the GUs are dominated by soft lithologies such as evaporites, clays, marls, and marly limestones, with abundant deformational structures. The GUs are a mixture of well-defined lithostratigraphic units and mélange-type units recognizable due to their unique features and deformation mechanisms.

Triassic materials are the most abundant unit in the GU, comprising nearly 70% of the total study area, and they are a key component in structural interpretations. The stratigraphic features of these materials are typically from the South Iberian Triassic [*Pérez-López*, 1991; *Pérez-Valera*, 2005; *Pérez-López and Pérez-Valera*, 2007], which constitutes the classic German-Andalusian facies of *Blumenthal* [1927]. In this regard, the attribution of these materials to specific, well-known stratigraphic units in other sectors of the Betic Cordillera helps to locate the origin of the materials. Specifically, the Triassic units in the GU correlate well with those located in areas within the Subbetic Zone and therefore do not correspond to Triassic units belonging to the Prebetic. Two main lithostratigraphic units can be differentiated: a detrital-evaporitic succession of Carnian-Norian age (Jaén Keuper Group) [*Pérez-López*, 1991] and a carbonate formation of Norian age (Zamoranos Formation) [*Pérez-López et al*., 2012]. In addition, these units are strongly deformed and their beds are frequently fragmented, constituting gypsiferous breccias or megabreccias. The gypsum units pass in depth to halite beds (Figure 3), corroborated by the briny water of small streams and drill cores. These gypsum breccia units are extensive and show abundant deformational processes, being included in a mélange-type unit described in the next section.

Strongly deformed units are also present in the GU, comprising pelagic marls and calcareous-marly sequences of Early Cretaceous and Late Cretaceous-Paleogene age, with several formations described in the Subbetic Zone in the Betic Cordillera recognized, especially the Capas-Rojas Formation [*Vera and Molina*, 1999]. Moreover, dismembered Jurassic carbonate units are present to a minor extent (Figure 3) but can also be attributed to several Subbetic Zone formations. Like the Triassic material, Cretaceous-Paleogene units show deformational features that can be interpreted as a mélange-type unit (described in the next section).

Neogene units lie unconformably over the GU, organized into three syntectonic and posttectonic sequences related to the deformational processes occurring at the front of the Betics (Figure 3). Due to their importance in the deformational history of GU, the age of Neogene units has been determined and accurated from new micropaleontological data. Sequences I and II are composed of mixed carbonate-siliciclastic successions of latest Oligocene-early Miocene and middle Miocene age, respectively, separated by a regional unconformity. Both sequences are extensively folded and thrust by tectonic processes that affect the GU (Figure 3) and can be partially correlated with the Castro del Río unit [*Roldán-García*, 1994; *Rodríguez-Fernández et al*., 2013]. Sequence III is composed of a late Miocene (Tortonian-Messinian) marly and calcareous sandstone succession, unconformably deposited over the GU and the two sequences described above, postdating the main tectonic events in the region (Figure 3), although deformation continued until the present as testified by seismic activity [*Pérez-Valera et al*., 2012]. This sequence III can be correlated with the first unit of the Guadalquivir Basin autochthonous infill in this sector, sequences A and B of *Sierro et al*. [1996], the Porcuna Unit [*Roldán-García*, 1994], or the Betica Depositional Sequence [*Riaza and Martínez del Olmo*, 1996].

4.1. Mélange Units

A significant part of GU is formed by rock bodies with an internal structure apparently chaotic, showing stratal disruption and mixing processes. It is common in the presence of metric to decametric blocks of different natures, both competent (limestones, sandstones, and volcanic rocks) and incompetent (shales, gypsum, marls, and marly limestones) rocks in a pervasively deformed clay-rich or gypsum-rich matrix. They display some stratal disruption mechanisms and deformational features and mostly have a mesoscopic, penetrative, block-in-matrix fabric. These features are usually described in meláng es and broken formations related to tectonic, sedimentary, and diapiric processes in different geodynamic settings [*Vannucchi and Bettelli*, 2010; *Festa et al*., 2012].

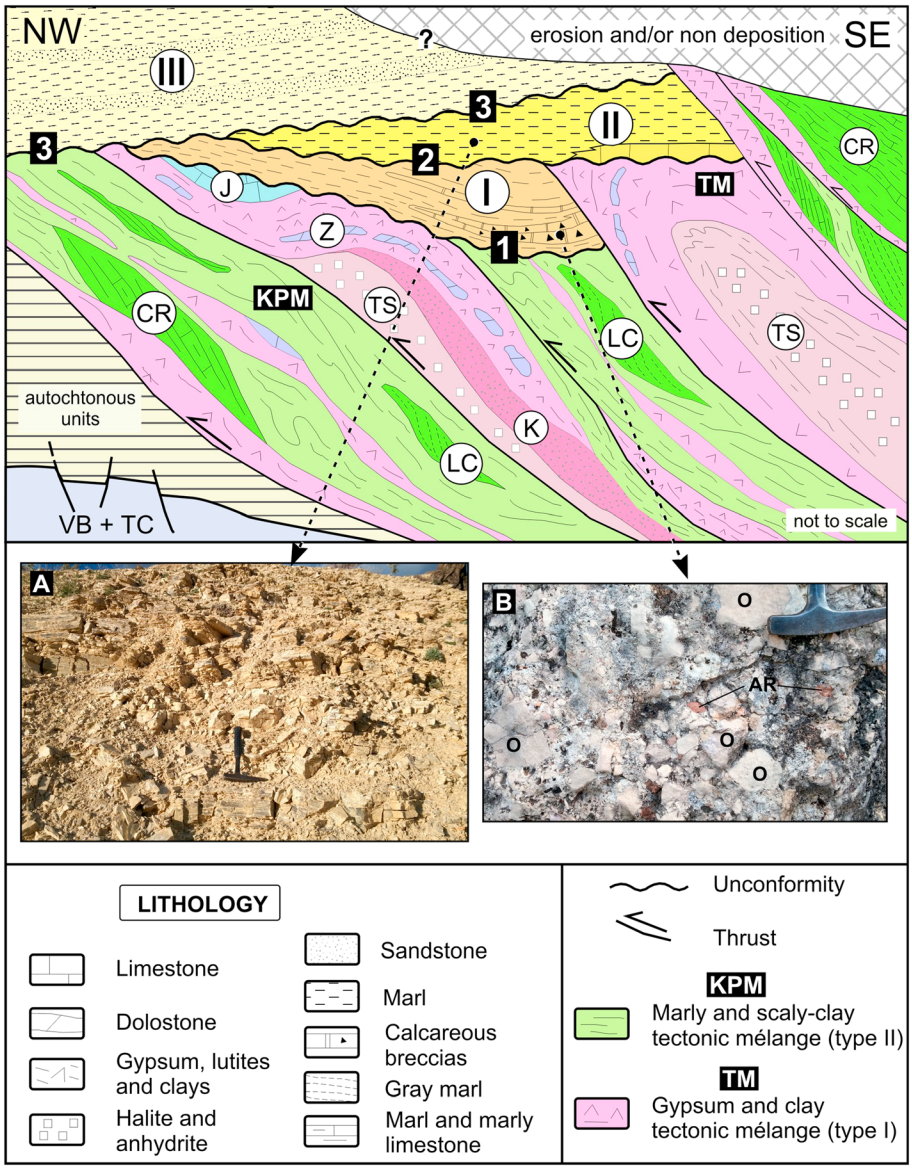

Figure 3. Conceptual model showing the relationship between the different lithostratigraphic and tectonic units in the north end of the Betic. TM: Triassic mélange (type I). KPM: Cretaceous-Paleogene mélange (type II). TS: Triassic Salt. K: Keuper units. Z: Zamoranos Formation. (Norian). J: Jurassic units. LC: Early Cretaceous units. CR: Capas Rojas Formation (Late Cretaceous-early Paleogene). I, II, and III: Neogene units. 1, 2, and 3: unconformities. IB: Variscan basement. TC: Tabular cover (Undeformed Mesozoic units). Not to scale. (a) Aspect of white pelagic marls and siliceous marls of the Unit II. Road from Torredelcampo to Villardompardo (geographical coordinates: 37.795104, −3.908839). (b) Detail of the carbonate breccias of Unit I. O: clasts of Middle Jurassic oolite limestone from Subbetic units. AR: clasts of Ammonítico Rosso Fm from the Jurassic of Subbetic Units. Puente del Villar locality (geographical coordinates: 37.826288, −3.991555).

Two mélange units occur in the GU, based on their composition and deformational features, and can only be differentiated on a mesoscopic, outcrop scale: (1) a gypsum-rich matrix mélange (type I), mainly composed of evaporite-bearing Triassic rocks, and (2) a clay-rich matrix mélange (type II), composed mostly of marls, marly limestones, and clay-rich rocks belong to units of Cretaceous-Paleogene age.

The type I mélange (Triassic mélange, TM, Figures 3 and 5) is composed of gypsum breccias with a variable amount of clays, including both competent and incompetent clasts of size ranging from millimeters to decameters, all belonging to the South Iberian Triassic units cropping out in the External Zones of the Betic Cordillera. Within the type I mélange appear decametric to hectometric stratigraphical successions of Jaén

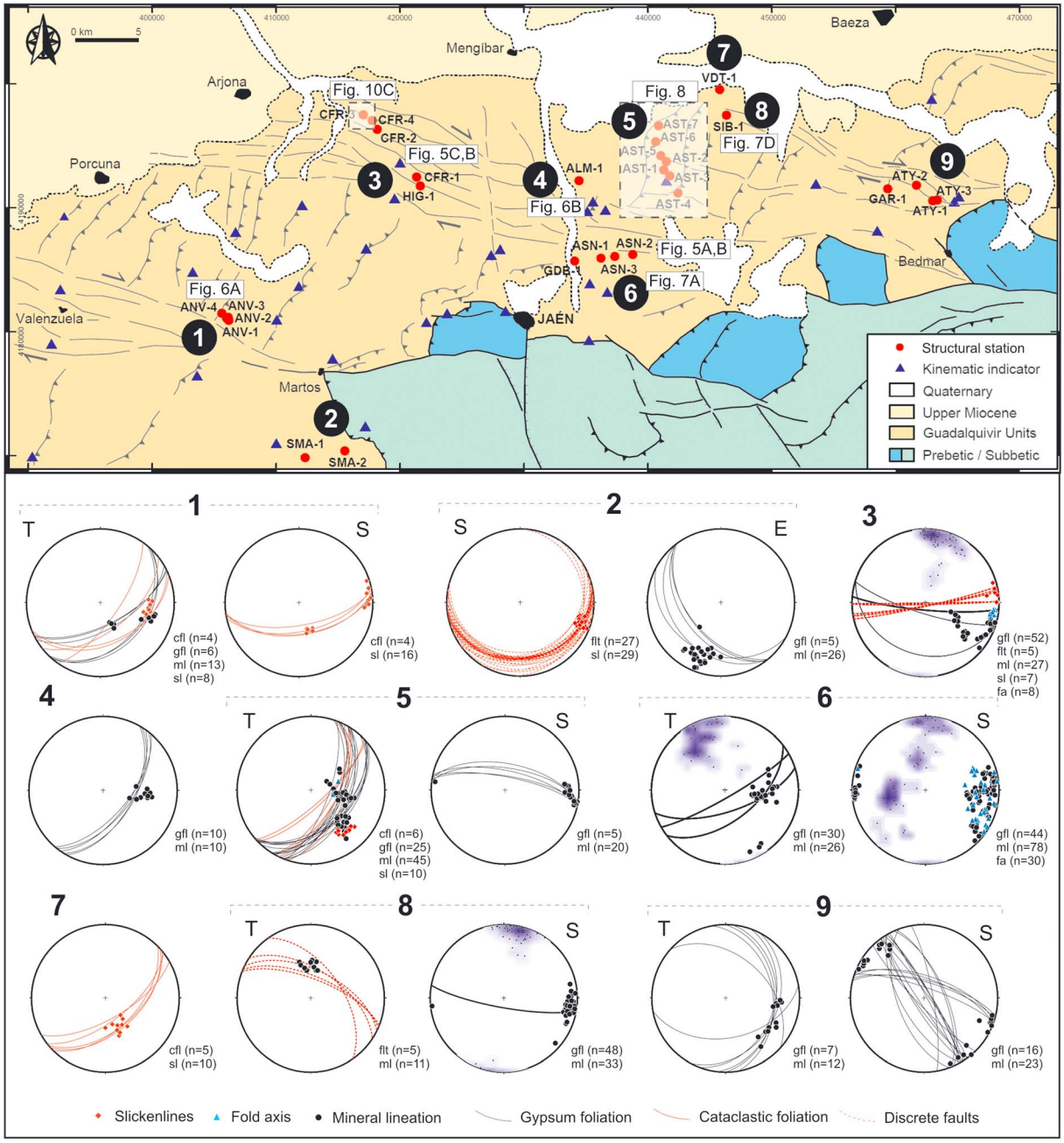

Figure 4. A: Simplified structural map showing location of the main structural stations and kinematic indicators. B: Stereo plots of the structural data by sectors. T: Thrust domain plot; S: Strike-slip domain plot; Ex: Extensional domain plot. cfl: Cataclastic P-foliation (continuous red great circles); gfl: gypsum foliation (black great circles); flt: discrete faults (dashed red great circles); ml: mineral lineation (black dots); sl: slickenlines (red diamonds); fa: fold axis (blue triangles). Great circles in bold: maximum average of gypsum foliation. Density contour of gypsum foliation poles is represented in violet.

Keuper Group, Zamoranos Formation and occasionally other units with some stratigraphic continuity (e.g., Jurassic blocks) (Figure 3). Non-Triassic material (e.g., Cretaceous-Paleogene pelagic marls) can be found as tectonic slices in this mélange unit, especially toward the contact with the type II mélange. The prominent structure of the type I mélange is a cataclastic foliation where rigid rock bodies are surrounded by a gypsum foliation (pseudobedding), showing clear boudinage and occasionally sigmoidal morphologies. Furthermore, in areas with more intense deformation, viscous-plastic mechanism produces gypsum tectonites. The tectonic fabric present in the gypsum breccias suggests that these brecciated units were produced ultimately by tectonic processes, although previous salt tectonic processes are inherited.

Moreover, the development of tectonic fabrics in the vicinity of thrusts or shear zones with consistent kinematic criteria confirms that tectonic processes are closely related with the formation of these units, allowing their designation as mélange [*Festa et al*., 2010, 2012] or tectonic mélange [*Vannucchi and Bettelli*, 2010].

The type II mélange (Cretaceous-Paleogene mélange, KPg, Figures 3 and 6) is composed of a mixing of metric to decametric disrupted rock bodies of Cretaceous-Paleogene stratigraphic sequences deriving from well-known, formally defined lithostratigraphic units of the Subbetic domain of the Betic External Zones. This formations are constitutes by clays, shales, marls, white and red marly limestones, bioclastic limestones, and turbiditic sandstones, containing abundant pelagic microfauna and macrofauna ranging from Early Cretaceous (Valanginian) to late Eocene. Within this type II mélange occur metric sheets of Triassic red clays and gypsum breccias. The type II mélange shows a penetrative rough cleavage in the clay-rich parts and blocks-in-matrix fabric in the marly limestone formations. Scaly cleavage are penetrative at mesoscale and microscale, with the presence of anastomosing shear zones showing polished surfaces where slickensides and P-Y-R_1 geometries can be used as kinematic indicators (Figures 4 and 6). Disrupted bodies made up of marls and marly limestones show a block-in-matrix fabric with lozenge-shaped boudins of marly limestones in a clayey marl matrix. Both matrix and clasts, of size ranging from millimeters to centimeters, commonly belong to the same stratigraphic sequence. This is particularly frequent in the red marls and marly limestones of Capas Rojas Formation (Figure 6c). Nevertheless, block-in-matrix fabric occasionally affects units belonging to other stratigraphic successions. All these features are consistent with the description of broken/dismembered formations or tectonites s. l. of *Vannucchi and Bettelli* [2010] or tectonosomes [*Pini*, 1999], although the term mélange can be applied for these units in a descriptive sense [*Festa et al*., 2012].

5. Structural Geology

The area's structural analysis has been conditioned by its mainly marly-evaporitic nature and intense farming, which relegates useful outcrops to gullies, recent road cuts, quarries, and landslides. Nevertheless, a sizeable group of outcrops with well-recognizable tectonic fabrics has revealed vertical shear zones that individualized several fold-and-thrust belts (Figure 4). Widespread ductile structures in the gypsum-bearing units (Triassic and mélange type I, Figure 5) coexist with brittle deformation in pelites and carbonate rocks (Figure 6). Kinematics deduced from fabric and discrete structures is very consistent, with dextral shear sense in the vertical strike-slip fault zones and a top-to-the-W or WNW sense in the thrusts (Figures 7a and 7b). We have also mapped a key sector of ~50 km^2 in order to describe how the thrusts are organized on a close-range scale and propose a realistic cross section from seismic profiles. Field observations have been completed by electrical resistivity tomography to depict the main structural styles of thrusts and wrench zones.

5.1. Mesoscopic Structures: Gypsum Fabrics and Scaly Clays

The GUs show a complete catalogue of deformation structures ranging from true S- and L-tectonites to breccias, including combined types such as foliated cataclasites. The type of deformation depends on the mechanical behavior of the lithology, and no relationship to the main structures that produce it (any specific thrust or transfer fault) has been found. In fact, ductile and brittle deformation with the same kinematics can be observed in sections only a few meters far.

The most important fabrics are represented by the S- and L-tectonites in the gypsum-bearing rocks. Gypsum fabrics containing kinematic criteria have scarcely been described in previous works [*Malavieille and Ritz*, 1989; *Jordan*, 1991]. Here gypsum ductile structures are common and contribute decisively to recognizing the region's tectonic organization. One type of L-tectonites comprises penetrative sheath folds depicted by fine pelitic intercalations (Figure 5a) or gypsum color changes. Locally, the fabric shows gypsum rod lineation (Figure 5d) with fold hinges. Gypsum fibers growing over fault planes are very abundant. When fault planes become penetrative, these result in a generalized planar-linear fabric, where direction and sense of transport can be identified (Figure 5b). Although late gypsum recrystallization seems to obliterate mineral lineations such as fibers (elongated grains and rods are not always evident), foliation and banding remain and are ubiquitous. Foliation and banding are discernible as millimeter to centimeter color changes due to reddish and greenish impurities and also by crystal size changes that give way to darker (smaller crystals) and lighter (larger crystals) bands. The tectonic nature of the foliation is evidenced by boudinaged levels of sandstone or dolostone (Figure 5e). Mineral fiber overgrowths in the pressure shadows in competent clasts are an additional valuable tectonic lineation visible in the field.

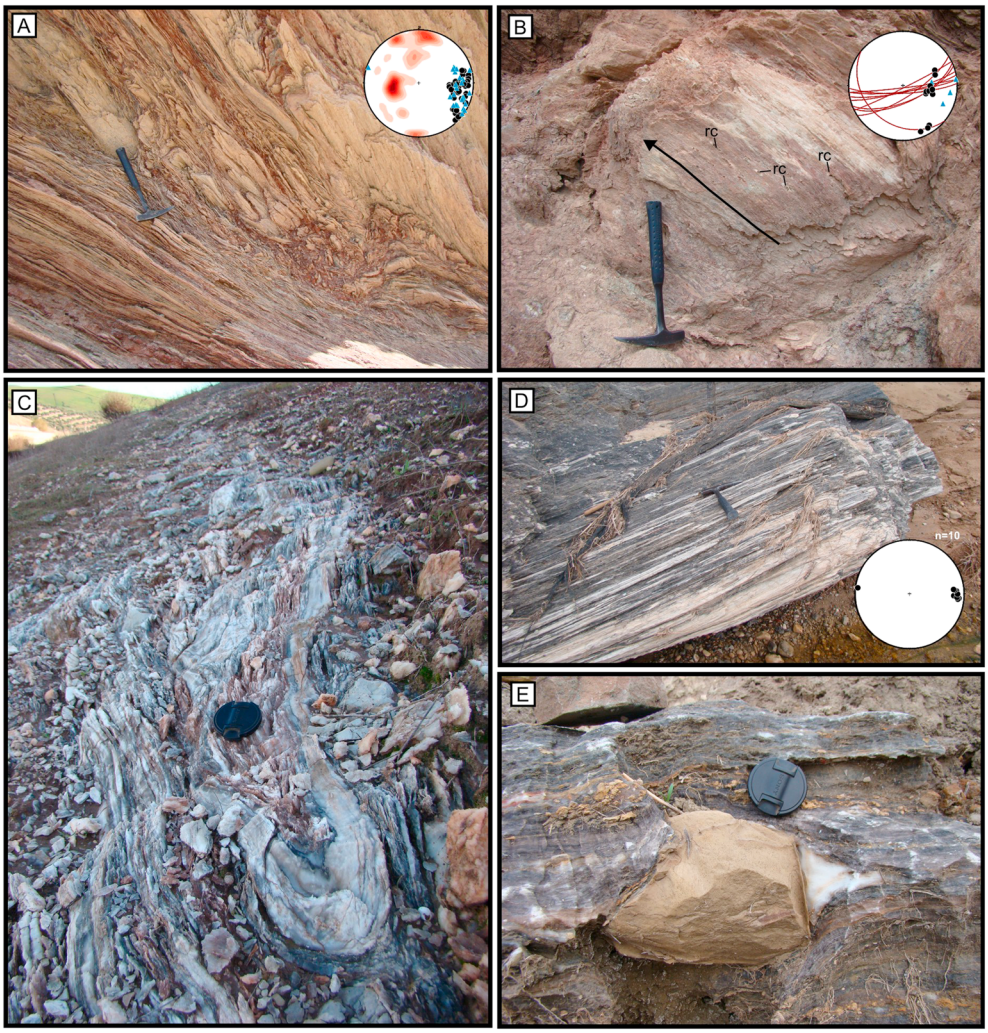

Figure 5. Mesoscopic structures in gypsum-bearing rocks of melánge type I unit. (a) Sheath folds in gypsum forming a penetrative lineation parallel to the folding axis. Stereo plots of ASN-2 station (blue triangles: sheath fold axes; black dots: mineral lineation of gypsum; density contour of gypsum foliation poles is represented in red). Location in Figure 4, Arroyo de la Salinilla. (b) Gypsum fibers growing in thrust planes. Note the position of rigid clast (rc) with small gypsum tails. Stereoplots of ASN-1 station (red great circles: cataclastic foliation; blue triangles: sheath fold axes; black dots: mineral lineation of gypsum). Location in Figure 4, Arroyo de la Salinilla. (c) Intrafoliar sheath fold of mesoscopic scale with a shear direction of N110E, congruent with the regional tectonic direction. Location in Figure 4, Carretera Fuerte del Rey-Higuera de Arjona. (d) Stretching lineation in gypsum. Stereoplot of AST-6 station (black dots: mineral lineation of gypsum). Location in Figure 8, Arroyo Salado de Torrequebradilla. (e) Dolostone clast between the gypsum foliation. Note the gypsum tails. Foliation is subvertical, N105E. Location in Figure 4, Fuerte del Rey.

Mineral lineations and tectonic foliations are present in both thrust and strike-slip shear zones (Figures 4 and 7). Sheath folds are more abundant in shear zones (Figure 4, stereographs 3 and 6) but are found occasionally in thrust fault zones (Figure 4, stereograph 5T). Tectonic foliation is sporadically deformed by tight, metric-scale folds (Figure 5c) whose axis is parallel to the main tectonic trend (Figure 4, stereograph 3). L-tectonites have no clear criteria to determine the shear sense; however, SL-tectonites have S-C structures that indicate the sense of transport.

Gypsum SL-tectonites from mélange type I show a continuous transition to cataclasites depending on the competent material/gypsum-matrix ratio. Larger marly or detritic content in the mix implies a relatively more disorganized fabric, which nevertheless has preserved broad banding. On the other hand, intensely sheared clay-bearing bodies give rise to a foliated cataclasite that incorporates a quasi-penetrative lineation formed

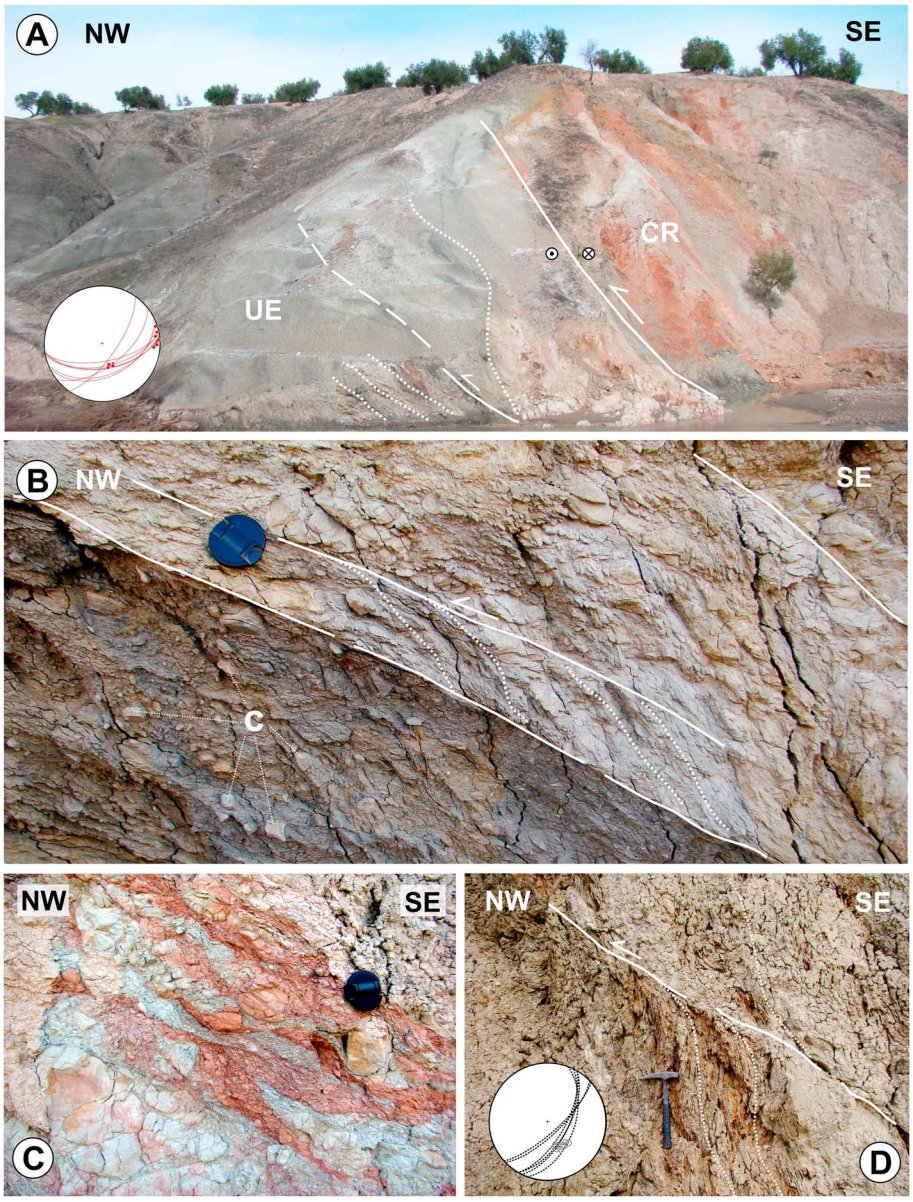

Figure 6. Mesoscopic structures in scaly clays and broken formations. (a) General view of the contact between the Capas Rojas Formation (CR) and Later Eocene rocks (UE), with the development of a penetrative scaly fabric. Stereoplot of ANV-3 Station (red great circles: cataclastic foliation; red diamonds: slickenlines). Location in Figure 4, Arroyo de las Nueve Vueltas. (b) Outcrop of mélange type II, showing a penetrative scaly or P-R fabric. Note the angular clasts (c) embedded in a clay-rich obscure matrix. Location in Figure 4, Arroyo Cadimo. (c) Scaly cleavage in Capas Rojas Formation. Location in Figure 8, Arroyo Salado de Torrequebradilla. (d) Penetrative scaly fabric in melánge type II unit showing P-R fabric. Stereoplot of AST-7 station (dashed great circles: scaly fabric; dots: slickenlines). Location in Figure 8, Arroyo Salado de Torrequebradilla.

by mineral (gypsum) slickenlines, clusters, and fibers on the foliation planes. Shear sense is deduced in the foliated cataclasites from asymmetric, rotated porphyroclasts, as well as slickenfiber congruous steps. The orientation of the foliation and lineation observed in SL-tectonites and foliated cataclasites are congruent at the outcrop and regional scale and are therefore represented together in the stereoplots in Figure 4.

Nonevaporitic units, mainly from mélange type II or clay-bearing gypsum-free Triassic layers, also exhibit pervasive deformation (Figure 6b), similar to those described in accretionary complex or mélange zones such as scaly clays or scaly shales [*Page*, 1963; *Abbate et al.*, 1970; *Vannucchi et al.*, 2003; *Vannucchi and Bettelli*, 2010]. These consist of anastomosed shear planes forming sigmoidal or symmetric lenticles. The

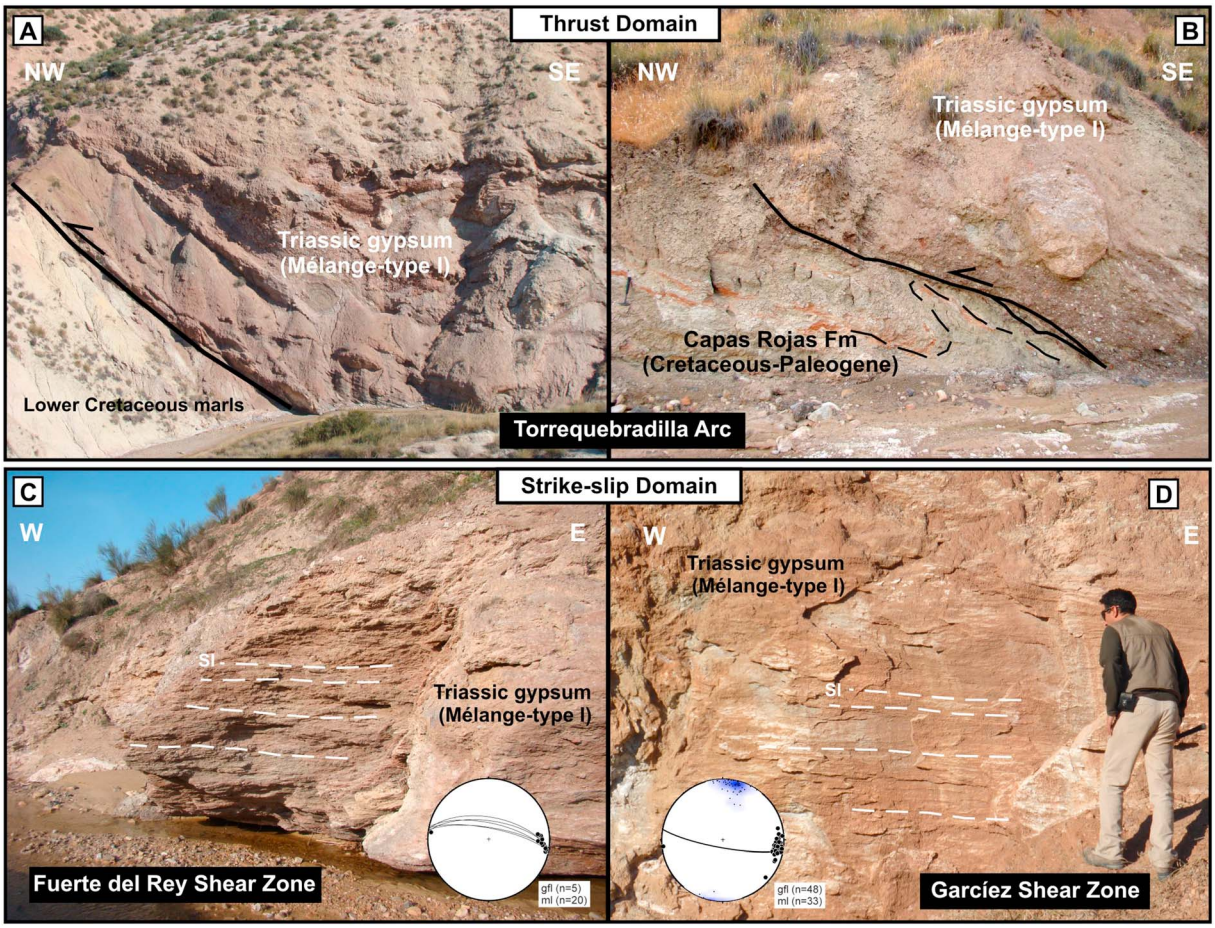

Figure 7. (a) Thrust of Triassic gypsum breccias (mélange type I) over Early Cretaceous pelagic marls of Subbetic origin. Gypsum fibers in the fault plane show a tectonic transport of N280E. Arroyo de la Salinilla, location in Figure 4. (b) Thrust of Triassic gypsum breccias (mélange type I) over Cretaceous-Paleogene Capas Rojas Formation of Subbetic origin. Arroyo Salado, location in Figure 8. (c) Subhorizontal stretching lineation in gypsum breccias (mélange type I) in a dextral shear zone. Orientation of lineation is N100E (AST-6 station). Arroyo Salado de Torrequebradilla, location in Figure 8. (d) Subhorizontal stretching lineation in gypsum breccias (mélange type I) in the dextral shear zone of Garcíez (GSZ). Orientation of lineation is N100E (SIB-1 station). Silleta de Barrera, location in Figure 4.

planes bounding the lenticles are slickensides that can be correlated with P-Y-R_1 planes from a cataclastic fabric (Figure 6b), known as P-R composite fabric [*Rutter et al.*, 1986; *Cladouhos*, 1999; *Takagi*, 1998]. The transport direction is marked by striations on the slickensides and shows no significant differences with those in the SL-tectonites (Figure 4). The P-R composite fabric indicates the sense of shear (Figure 6b). Cataclastic fabrics may also show the shear sense through a relative geometric offset of contacts and sedimentary markers (Figure 6c). Drag folds produced by out-of-sequence shear planes (Figure 6d) are other common shear sense criteria.

Faults frequently bound or are inside shear zones with the penetrative fabrics described above, either alone or as part of fault zones. Faults present slickensides with striations and slickenfibers congruent with the rest of the kinematic indicators. Site 2 from Figure 4 shows nearly E-W fault planes with strike-slip striations. On the other hand, site 8 (Figure 4) exemplifies a fault zone with oblique back thrust with a top-to-the-SE sense of shear. Fibrous vein fillings do not have a predominant orientation. Nevertheless, in some outcrops the fibers show preferred NNE-SSW growth, independent of the vein wall orientation, that is, perpendicular to the thrust.

5.2. Key Sectors of the Guadalquivir Units

The Torrequebradilla area is a representative section of the thrust belts that configure the southern margin of the Guadalquivir (Figure 8). The detailed geological map shows the frontal area of the so-called

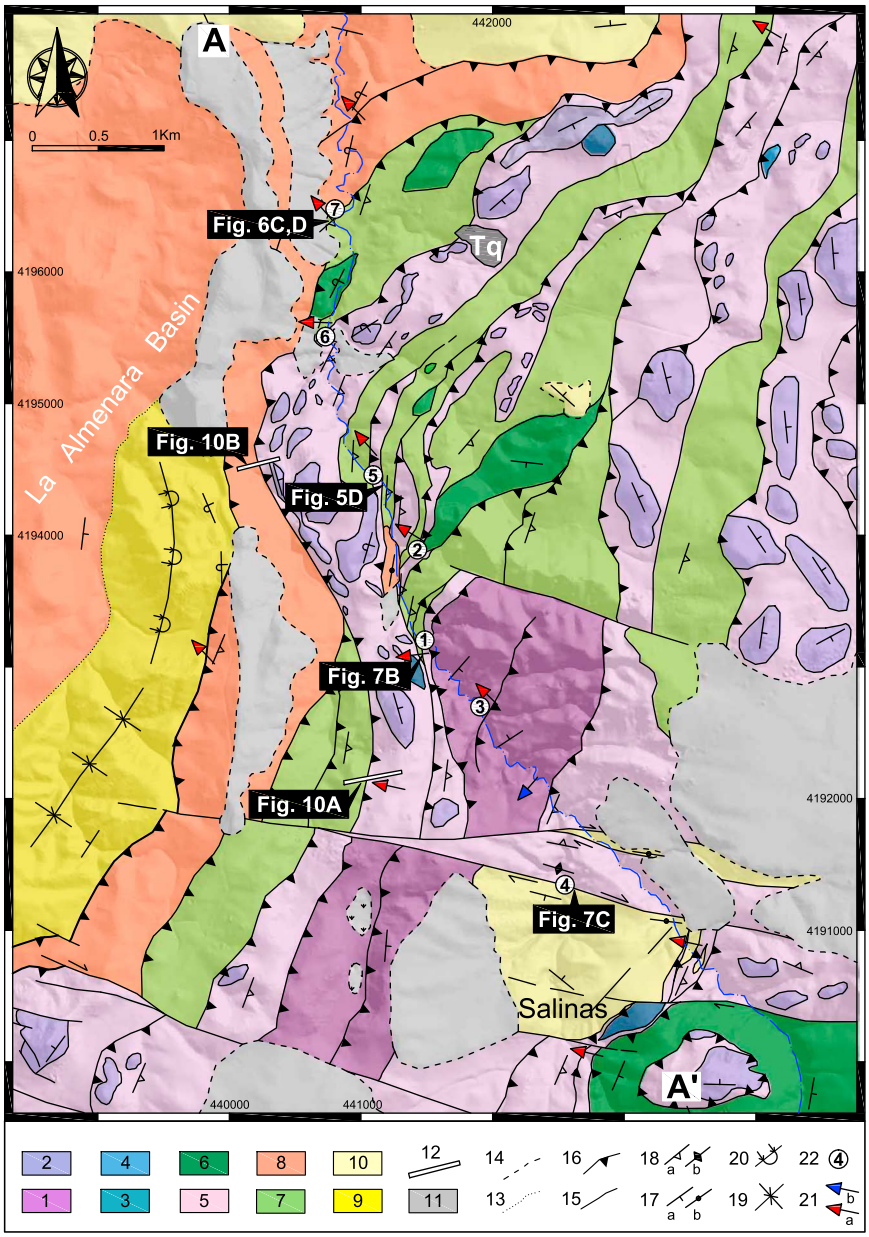

Figure 8. Geological map of Torrequebradilla area. Position in Figure 4. 1: Variegated sandstones, lutites, and gypsum (Keuper facies, Carnian). 2: Dolostones (Zamoranos Formation, Norian). 3: Subvolcanic rocks (ophites, Triassic). 4: Limestones ((Early Jurassic). 5: Gypsum breccias (mélange type I). 6: Marls and marly limestones (Late Cretaceous-Paleogene). 7: Blocks-in-matrix mélange (mélange type II). 8: Clays and sandstones (latest Oligocene-Burdigalian). 9: Siliceous marls and marly limestones (Burdigalian). 10: Marls and sandstone (Serravalian). 11: Quaternary deposits. 12: Tomography profiles. 13: Concordance. 14: Unconformable contact. 15: Tectonic contact. 16: Thrust. 17: (a) Strike and dip of bedding and (b) subvertical. 18: (a) Foliation strike and dip and (b) subvertical. 19: Syncline. 20: Anticline. 21: (a) Compressional slip vector (hanging wall) and (b) extensional slip vector (hanging wall). 22: Structure measurement station. Tq: Torrequebradilla town.

Torrequebradilla Arc (TQA, Figure 4), which thrusts over the Almenara Basin, an early-middle Miocene sedimentary subbasin to the west (Figure 8).

The thrust system is composed of several sheets of varied nature. The most extensive are a pair of mélange-type I sheets at bottom and mélange-type II at top (Figures 8 and 9). However, kilometer-size blocks inside the mélange and fault-limited horses of the original lithologies can be recognized (e.g., Triassic Keuper,

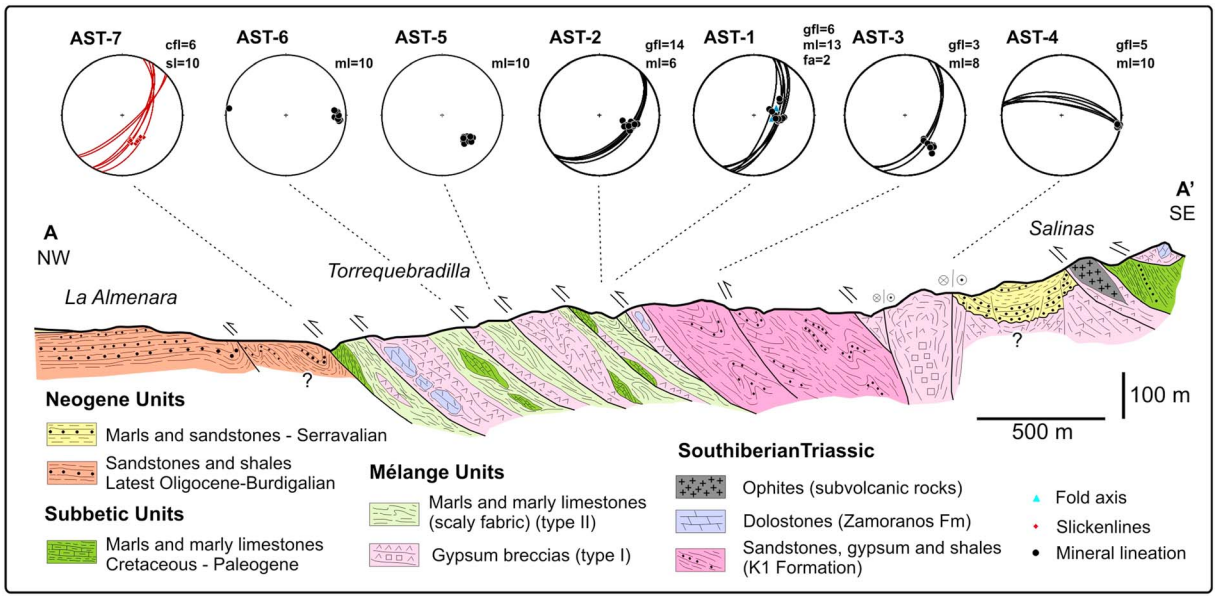

Figure 9. Geological section of Torrequebradilla sector and stereoplots of structural data. Position is indicated in Figure 8 (A-A′). cfl: cataclastic P-foliation (continuous red great circles); gfl: gypsum foliation (black great circles); ml: mineral lineation (black dots); sl: slickenlines (red diamonds); fa: fold axis (blue triangles).

Zamoranos Formation and subvolcanic rocks, Jurassic limestones, and Cretaceous-Paleogene marly limestone). In contrast, the Almenara Basin consists of subhorizontal late Oligocene to middle Miocene sediments hundreds of meters from the thrust front, although they are sliced and folded close to the contact with the mélange units, achieving vertical and reverse dips.

The mapped thrust system forms an imbricate fan (Figure 9) of 10 main slices dipping 40–50° southeast and describing an arcuate salient (Figure 8). Folds and thrust have constant NW vergence throughout the area. Thrusts trend NNE-SSW, except at the salient, where fault strikes are deflected up to 45° counterclockwise. Fold axial traces in the early Miocene sediments run parallel to the frontal thrust. The TQA is limited by two major strike-slip fault zones general trending E-W (Figure 4). The Fuerte del Rey Shear Zone (FRSZ), south of the TQA, can be followed for more than 40 km, with a width that can exceed 5 km. The FRSZ is characterized by subvertical fault sets that juxtapose elongated rock bodies at different scales (kilometric to metric). In fact, the FRSZ has gypsum tectonites and P-R fabrics with subvertical foliation and E-W subhorizontal stretching lineation (AST-4 station, Figures 4, 7c, and 9). Where the sense of shear can be observed, it is always dextral.

Miocene sediments are involved in the strike-slip fault systems. Isolated outcrops of middle Miocene (Early Serravalian) rocks are visible above the TQA imbricate fan. They consist of a set of laminated, turbidite-like sandstones with layers of sedimentary breccias of Triassic dolostones and Jurassic limestones, siltstones, and marls. Nevertheless, sediments reach noticeably greater thickness between two strike-slip faults from the FRSZ (Salinas, Figure 8), suggesting that vertical transtensional movements controlled sedimentation at that time in the strike-slip shear zones. Sediments lie unconformably over type I mélange units and thus postdate the emplacement of these tectonic units. Nevertheless, the Salinas Serravalian sediments are folded normal to the strike-slip fault traces and are also faulted with the same trend and vergence as the thrust system (Figures 8 and 9). Miocene beds near the main fault zones are subparallel to them (E-W to N110°E) with vertical dips.

5.3. Geophysical Imaging of Main Structures

5.3.1. Electrical Resistivity Tomography

Two electrical resistivity tomography profiles have been carried out across the Torrequebradilla thrust system (Figures 10a and 10b) and the Fuerte del Rey Shear Zone (Figures 10d). These profiles complement the field data and corroborate the structural style and geometry in key sectors of the study area that are intensively cultivated and show bad outcropping conditions.

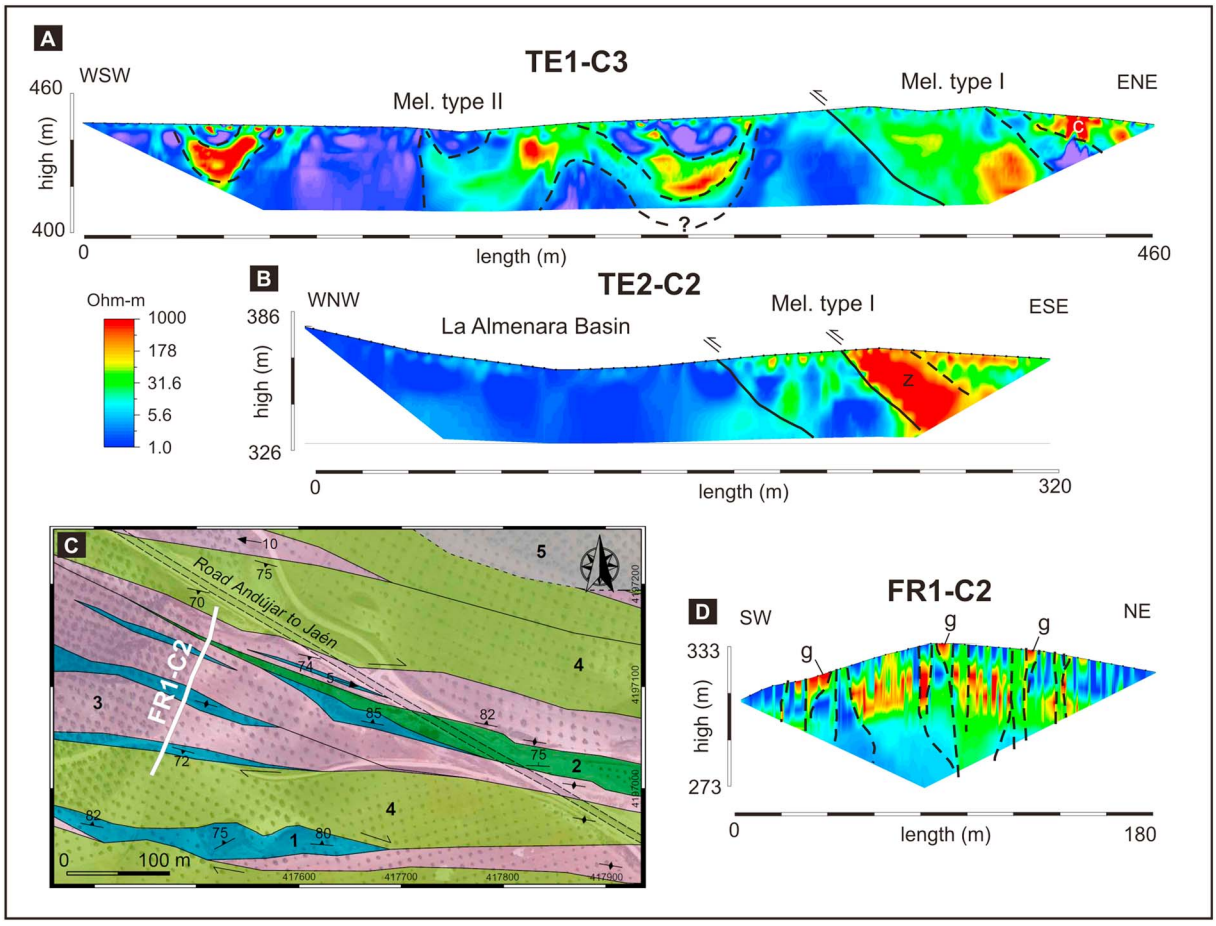

Figure 10. (a) Tomography profile TE1-C3 and its interpretation. c: Carbonates. Location of profile in Figure 8. (b) Interpretation of the TE2-C2 tomography profile in Figure 8. z: Zamoranos Formation. (c) Detailed geological map of a sector in the Fuerte del Rey Shear Zone, with position of FR1-C2 profile. Location in Figure 4. Position of tectonic station CFR-3 is also indicated. 1: Foliated gypsum (Keuper facies). 2: Early Cretaceous pelagic marls and marly limestones. 3: Gypsum breccias (mélange type I). 4: Scaly clays and broken formations (mélange type II). 5: Quaternary deposits. (d) Tomography profile FR1-C2 (location in Figure 10c) and its interpretation. g: Gypsum.

Profile TE1-C3 (Figure 10a), located in the Torrequebradilla key sector (Figure 8), shows a folded internal structure inside a mélange type II slice and an east dipping thrust in the contact between mélange type I and II, not recognizable at surface. Folds in the GU are only recognizable as large-scale structures, as can be seen in the N-S fold observed in the Miocene of Almenara Basin (Figure 8) and deduced by geological mapping. Nevertheless, in this profile folds can be traced following medium-high resistive materials (probably marly limestones) of the mélange type II. Profile TE2-CE2 (Figure 10b) is located to the north of the above described (Figure 8), in the contact of the Guadalquivir Units (TQA) with the Almenara Basin. The profile cut across materials of high-contrast resistivity: high-resistivity dolostones of Zamoranos Formation (Triassic) and very low resistivity of clays of the Oligo-Miocene unit (Almenara Basin). The results indicate the east dipping of the frontal thrust depicted by a body of the Zamoranos Formation (Z, Figure 10b) with hanging wall flat geometry. The east dipping thrust corroborates the west vergence of the TQA obtained from the kinematic data available in this sector (Figures 4, 8, and 9). Moreover, to characterize the lateral strike-slip shear zones, one profile (FR1-C2) has been made in the Fuerte del Rey Shear Zone (FRSZ). Figure 10c shows a detailed map of a FRSZ sector (location in Figure 4), where few subvertical slices only a few meters in width can be differentiated. The electrical resistivity tomography transverse to the strike (profile FR1-C2, Figure 10d) suggests a larger number of vertical rock bodies with a limited continuity in depth that would draw an anastomosed pattern in 3-D.

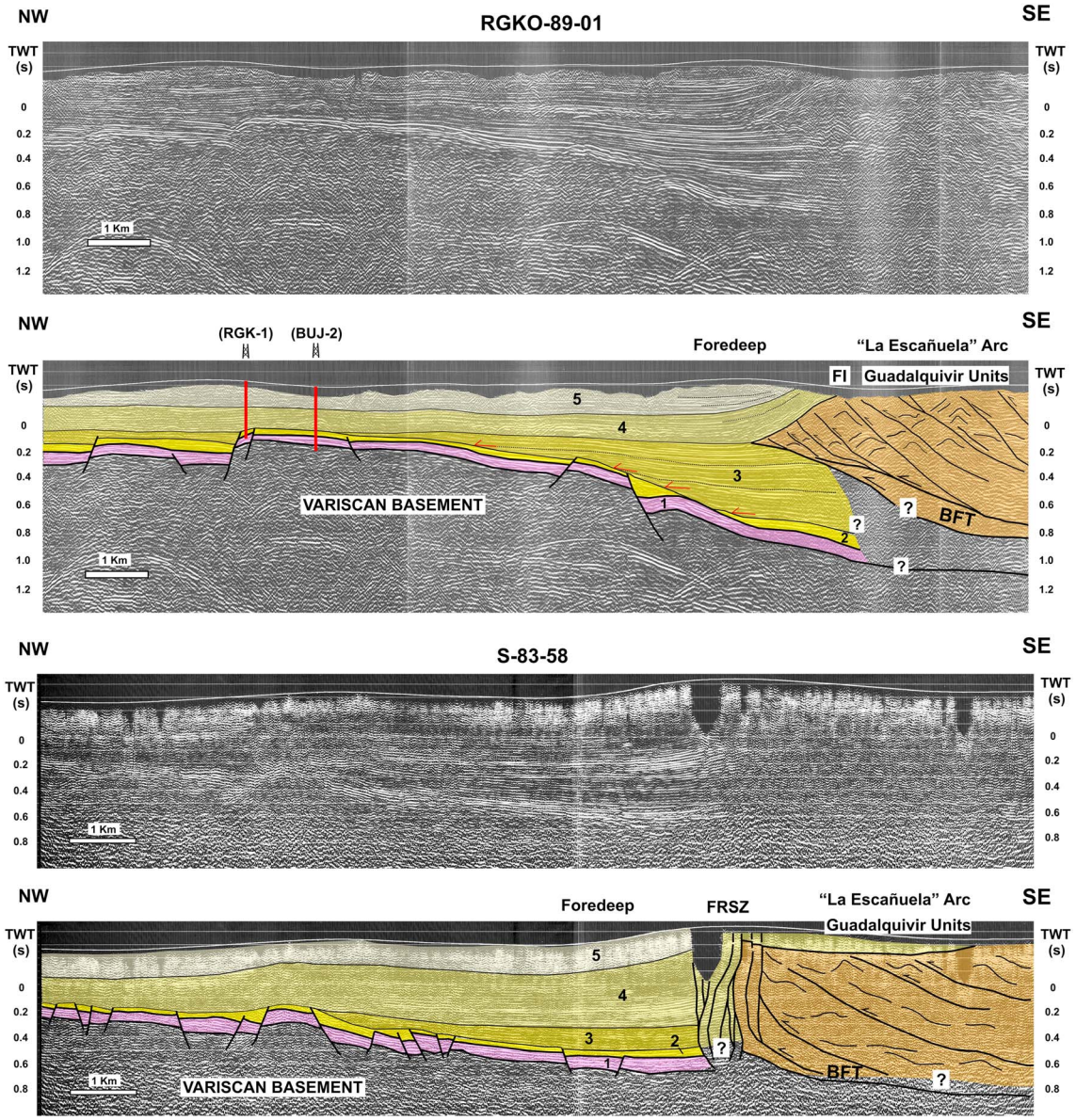

Figure 11. Seismic lines RGKO-89-01 and S83-50 and their interpretation. 1: Triassic (Tabular Cover). 2: Arenas del Guadalquivir Formation-Tortonian. 3: Unnamed unit-Tortonian. 4: Arenas del Guadalquivir Formation-Late Tortonian. 5: Porcuna calcarenites-Messinian. FI: Frontal Imbricates. FRSZ: Fuerte del Rey Shear Zone. BFT: Betic Floor Thrust. Location of the profiles in Figures 2 and 12.

5.3.2. Seismic Lines

Two seismic lines have been selected and interpreted in order to illustrate (1) the deep structure of thrusts and strike-slip systems of the Guadalquivir Units (geometry, thickness, and structural style); (2) the deep of the Paleozoic Variscan basement, the thickness and structures of the Mesozoic Tabular Cover, and the autochthonous infill of the foreland basin; and (3) the geometric relationship between the Guadalquivir Units and the Guadalquivir foreland basin.

RGKO-89-01 and S-83-58 lines are medium-quality seismic lines and show chief structures at the contact of the GU with the Guadalquivir foreland basin. RGKO-89-01 is the westernmost seismic line in the study zone (see the position in Figures 2 and 12). The line comprises the northwest end of the GU and their interaction with the foreland basin through the Escañuela Arc (ECA) (Figure 12). It can be recognized as a set of southeast dipping thrusts that form an imbricate system over the foredeep through a main basal thrust (Betic Floor Thrust, BFT, Figure 11). The frontal position and the imbricate geometry of the GU correlate well this

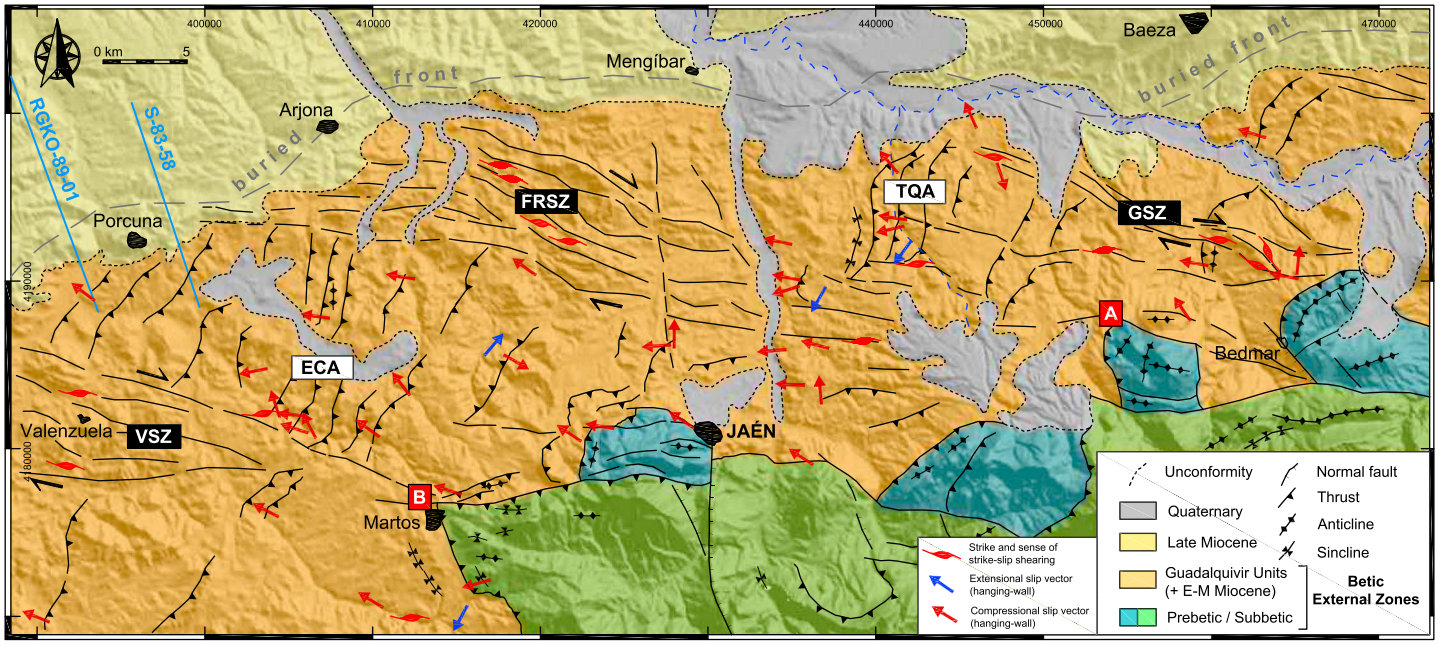

Figure 12. Structural map of the north end of the Betic orogen in the Jaén area, with location of seismic lines. TQA: Torrequebradilla Arc. ECA: La Escañuela Arc. GSZ: Garcíez Shear Zone. FRSZ: Fuerte del Rey Shear Zone. VSZ: Valenzuela Shear Zone. Points (A) and (B) indicate curvature points in the mountain front. See further explanation in the text.

structure with the frontal imbricate slices described by *Fernàndez et al*. [1998] in western parallel lines. Also, folds can be recognized inside of the GU, structures that fit well with the shortening and deformation during the emplacement of GU toward the WNW.

S-83-58 line is located 7 km east to the previous seismic line, but in this case crossing the FRSZ (Figures 2 and 12), which marks the end of the GU in this sector. The line shows the sharp, subvertical contact between the GU and the foredeep of the autochthonous foreland basin. The geometry and structural style of the FRSZ can be deduced from the presence of more than 1 km length of subvertical, east and west dipping faults, affecting to the foreland basin units (Figure 11). To the SE, the presence of disorganized seismic facies is indicative of the evaporite-bearing units that compose the GU, mainly Triassic and mélange type I, being difficult to see structures as folds and thrusts so clear than in the previously described line.

Information from two nearby wells (RGK-1 and BUJ-2) helps to interpret the acoustic basement and the five seismic units differentiated on the profiles within the Guadalquivir foreland basin (Figure 11). The acoustic basement correspond to the Variscan basement, drilled in BUJ-2 well, which is found at 550 m depth, getting deeper toward the southeast under the basal thrust of the GU. Above the acoustic basement, Unit 1 is located unconformably over the basement and belongs to an 80 to 150 m thick Triassic sequence made of sandstone red beds (Tabular cover). Unit 2 is composed of a Miocene basal member of coarse sandstones and calcarenites correlated with the Arenas de Base Formation of Tortonian age [*Riaza and Martínez del Olmo*, 1996; *Sierro et al*., 1996]. This unit predates the normal subsiding faults affecting Variscan basement and Triassic beds. Unit 3 is located in the southeast part of the lines and comprised a well-defined fan sequence of foredeep sediment onlapping the outer edge of the basin. The thickness of this unit ranges from more than 600 ms two-way traveltime to 0 ms, decreasing toward the northwest whereby it is not drilled in the wells. Meanwhile, Units 4 and 5 are well constrained and completely drilled in both wells. Unit 4 is composed of sandstones with pelagic marls, 220 m thick that are correlated with the Arenas del Guadalquivir Formation, Tortonian in age [*Castelló-Montori et al*., 1972; *Riaza and Martínez del Olmo*, 1996; *Sierro et al*., 1996]. Finally, Unit 5 corresponds to calcareous sandstones correlated with the Calcarenitas de Porcuna Mb of Latest Tortonian to Early Messinian age [*Sierro et al*., 1996; *Martínez del Olmo and Martín*, 2016].

5.4. Major Tectonic Structures: Curved Thrust Belts and Lateral Shear Zones

The alternations of curved thrust belts (arcuate thrust systems) limited by strike-slip fault zones described above are recognizable throughout the study area (Figure 4) at the cartographic (Figure 12) and outcrop scales

(Figure 7). The new regional cartography shows persistent N-S to NNE-SSW arcuate thrust systems (called arcs in a simplified form) bounded by dextral strike-slip fault zones, with a predominant direction of transport ranging from E-W to ESE-WNW (Figure 12). Three main strike-slip fault zones (termed, from northeast to southwest, the Garcíez Shear Zone (GSZ), Fuerte del Rey Shear Zone (FRSZ), and Valenzuela Shear Zone (VSZ)) differentiate two main thrust systems: the Torrequebradilla Arc (TQA) and the Escañuela Arc (ECA) (Figure 12).

The slip sense of thrust in the TQA and ECA is determined mainly from gypsum fibers growing in the thrust fault planes (Figure 4) that indicate a hanging wall movement toward W-WNW. Independently of the fault plane strike, two families of thrust directions can be recognized (Figure 4): most lineations are grouped between N085° and N120°, with a plunge of 60–25°, although some thrusts show a NW sense of shear (32°–N139° ± 7° in trend and plunge).

The dextral shear zones separating the arcs (GSZ, FRSZ, and VSZ) are composed of hectometric- to kilometric-wide subvertical tectonic contacts between the GU. The relationship between planar structures (penetrative foliation or discrete faults) and lineations inside the shear zones is complex and diverse. The most common situation consists of vertical E-W (N100°) planes with a lineation plunging 0–10° toward the east, but some low-dipping planes also occur (compare GSZ plot 9 with FRSZ plot 3 in Figure 4). When gypsum S-L tectonites are predominant, cataclastic foliation inside the shear zone can be folded around an axis that coincides with the local shear direction (Figure 4, plot 3 from FRSZ). Vertical Riedel planes with respect to the N100° regional trend are found occasionally (Figure 4, plot 8 from GSZ) and show horizontal NW-SE trending lineations with a consistent dextral shear sense. A single plane or site inside a shear zone can present two approximately orthogonal lineation sets (Figure 4, plots 1 and 8); one of the sets corresponds to the regional E-W strike-slip displacement, while the other one implies a north or south reverse component, thus revealing a transpressional regime, at least locally.

The deep structure of the GU is hard to recognize in the existing seismic profiles (see location in Figure 2) because most of them were made highly oblique to the trend of the thrust. However, the RGKO-89-01 line (at the west end of the ECA) shows the imbricate fan dipping southeast and thrusting over the foredeep basin (Figure 11). The ECA and TQA frontal edges should have a similar imbricate geometry, although the ECA has thicker sediments below the sole fault. The RGKO-89-01 line shows clear evidence of well-developed folding inside the ECA units, which have been observed at other scales in the outcrops and via electrical resistivity tomography (Figure 10a). In addition, the RGKO-89-01 line establishes a partial timing for the thrusting, since the main basal thrust finally is emplaced above the Seismic Unit 3 (Tortonian). The Arenas del Guadalquivir Formation (Late Tortonian) sealed this event although a progressive unconformity affecting this last formation and Calcarenitas de Porcuna (Messinian) indicates that movements were active at that time (Figure 11). The vertical organization from the strike-slip zones has been observed in seismic line S-83-58, at the west end of the FRSZ (Figure 11). The profile shows the abrupt contact between the GU and the late Miocene units from the foredeep of the autochthonous basin, affecting even the Arenas del Guadalquivir Formation. In the south border of the FRSZ faults dips at the NNE, while in the north dipping is to the SSW, suggesting a double vergence for the FRSZ. Also, the topographic elevation over the shear zone (Figure 11) can be related with the uplift of this structure. Therefore, the geometry and structural style of FRSZ could be interpreted as a positive-flower structure.

6. Discussion

6.1. Tectonic Interpretation and Kinematics of the Northern Betic Front

An exhaustive exam of the study area has revealed that a large amount of tectonic structures mainly in Triassic evaporites show nonchaotic deformation. The new structural data, the review and remapping of the area, and the redefined lithostratigraphic framework, together with the reinterpreted seismic lines, are consistent with the existence of an evaporite-bearing accretionary complex at the front of the Betic Cordillera, namely, the Guadalquivir Accretionary Complex (GAC).

The main features supporting this interpretation are the following:

1. The existence of a wedge-shaped, large-scale body, as seen in seismic lines (Figure 11), showing a main basal thrust, equivalent to the Betic Floor Thrust (BFT) defined by *Guezou et al.* [1991], over autochthonous Neogene sediments of the Guadalquivir Basin. The ramp geometry of the BFT, dipping gently southeast, is

consistent with the advance of a tectonic body that displays imbricate slabs of accreted units in its frontal part over a décollement (frontal imbricates, Figure 11), as previously interpreted by other authors [*Fernàndez et al*., 1998; *Ruiz-Constán et al*., 2012].

2. The well-defined structure of the GAC, with a combination of predominantly northwest verging, thrust arcs with almost perpendicular lateral shear zones, which are comparable with the structure of numerous accretionary complexes [*Davis et al*., 1983; *Sample and Fisher*, 1986; *Platt*, 1990; *Schlüter et al*., 2002].
3. The existence of a lithostratigraphic framework in which the GUs are large, allochthonous units (stratigraphically recognizable and mélange-type units) of Subbetic origin that show pervasive tectonic structures kinematically consistent with the emplacement of an accretionary body advancing toward the northwest. Moreover, the occurrence of syntectonic late Oligocene to middle Miocene marine sediments above the GU is typical of mobile basins (piggyback basins) forming during the successive migration and emplacement of an accretionary complex [*Ori and Friend*, 1984; *Huyghe et al*., 1999; *Chiang et al*., 2004].

Additionally, the abundance of evaporites in the GU, and its implication in the deformation of the Betic front, makes the GAC an unusual type of accretionary wedge in which evaporites do more than influence the structural style of the accretionary complex, as occurs in numerous orogens in the world [*Davis et al*., 1983; *Davis and Engelder*, 1985; *Jaumé and Lillie*, 1988; *Coward et al*., 1999; *Bahroudi and Koyi*, 2003] and in analogous experimental examples [*Letouzey et al*., 1995; *Costa and Vendeville*, 2002]. Instead, here the evaporites are implicated and form most of the accretionary complex, together with other incompetent lithologies such as clays, shale, and marls. This feature may be due to the extrusion of a large plastic mélange body, previously set as allocthonous salt sheets during the passive margin stage in the South Iberian paleomargin [*Flinch et al*., 1996; *Flinch*, 2003], then deformed and accreted by the westward advance and collision of the Alboran Domain, which gave rise to the Gibraltar Arc during the Neogene [*Balanyá and García-Dueñas*, 1987; *Platt et al*., 1995; *Balanyá et al*., 2007]. In this process, an evaporite-/clay-bearing body is expulsed (favored by its plastic rheological properties) and forms a frontal mélange during the collision, which is structured as a low-angle accretionary wedge fringing the central and western Betics. In the Gulf of Cádiz, the offshore part of the GAC, the accretionary wedge hypothesis has been widely described based on seismic data [e.g., *Gutscher et al*., 2009; *Duarte et al*., 2011].

The dominant WNW sense of tectonic transport observed in the thrusts (top to the N290°E) is slightly farther westward than in previously published works on the Subbetic [*Platt et al*., 1995; *Pedrera et al*., 2012], but similar to the Prebetic Cazorla Arc [*Guezou et al*., 1991; *Platt et al*., 2003] and Campo de Gibraltar domains [*Balanyá et al*., 2007]. In this respect, a west dominated vergence of N-S striking compressive structures (folds and thrusts) accompanied by roughly E-W dextral lateral strike-slip faults has been described in all the Betic domains [e.g., *Sanz de Galdeano*, 2003; *Crespo-Blanc and de Lamotte*, 2006; *Pérez-Valera et al*., 2011a, 2013; *Barcos et al*., 2015].

The N110°E dextral shear zones defined (GSZ, FRSZ, and VSZ, Figure 12) are almost parallel to the shortening and can therefore be considered as transfer zones [*Harding et al*., 1985; *Calassou et al*., 1993]. One of the particularities of the study sector is that these transfer zones are wider and longer than the observed thrust arcs, which is unusual compared to typically described ones [*Macedo and Marshak*, 1999; *Ruh et al*., 2013]. Nevertheless, it should be considered that these shear zones connect the main arcs of the Betics (Cazorla and Gibraltar), and therefore, the TQA and ECA thrust systems are somewhat secondary arcs accommodating only a minor part of the total transport throughout the area. On the other hand, the special characteristics of the GU conferred by the prevailing plastic-evaporitic material helps the branching of the shear zones, as occurs in orogens with a salt-bearing, ductile substrate, which commonly develop potentially diapiric salt walls and stocks in the transfer zones [*Cotton and Koyi*, 2000].

The structural trend of the GAC, observed in the study sector, suggests a main WNW-ESE shortening direction. However, a significant number of thrusts/reverse faults in the GAC have movements of the hanging wall toward the NW, north, or even south (e.g., VDT-1, SIB-1, and ARG-2 stations, Figure 13b, indicating N-S shortening. This is corroborated by the rotation of thrust strikes and axial fold traces from NNE-SSW to NE-SW and even ENE-WSW, for example, in the Torrequebradilla sector (Figure 8). Folds are commonly E-W directed inside the shear zones. This N-S shortening can be explained by three causes or a combination of them: (1) curved thrust-and-fold structures, (2) strain partitioning in a transpressive context, and (3) variations in the direction of compression over time. Arc-shaped thrust structures have been identified in the GAC, well represented in the Torrequebradilla Arc (Figures 8 and 12), where there is a variation of 40° in the slip

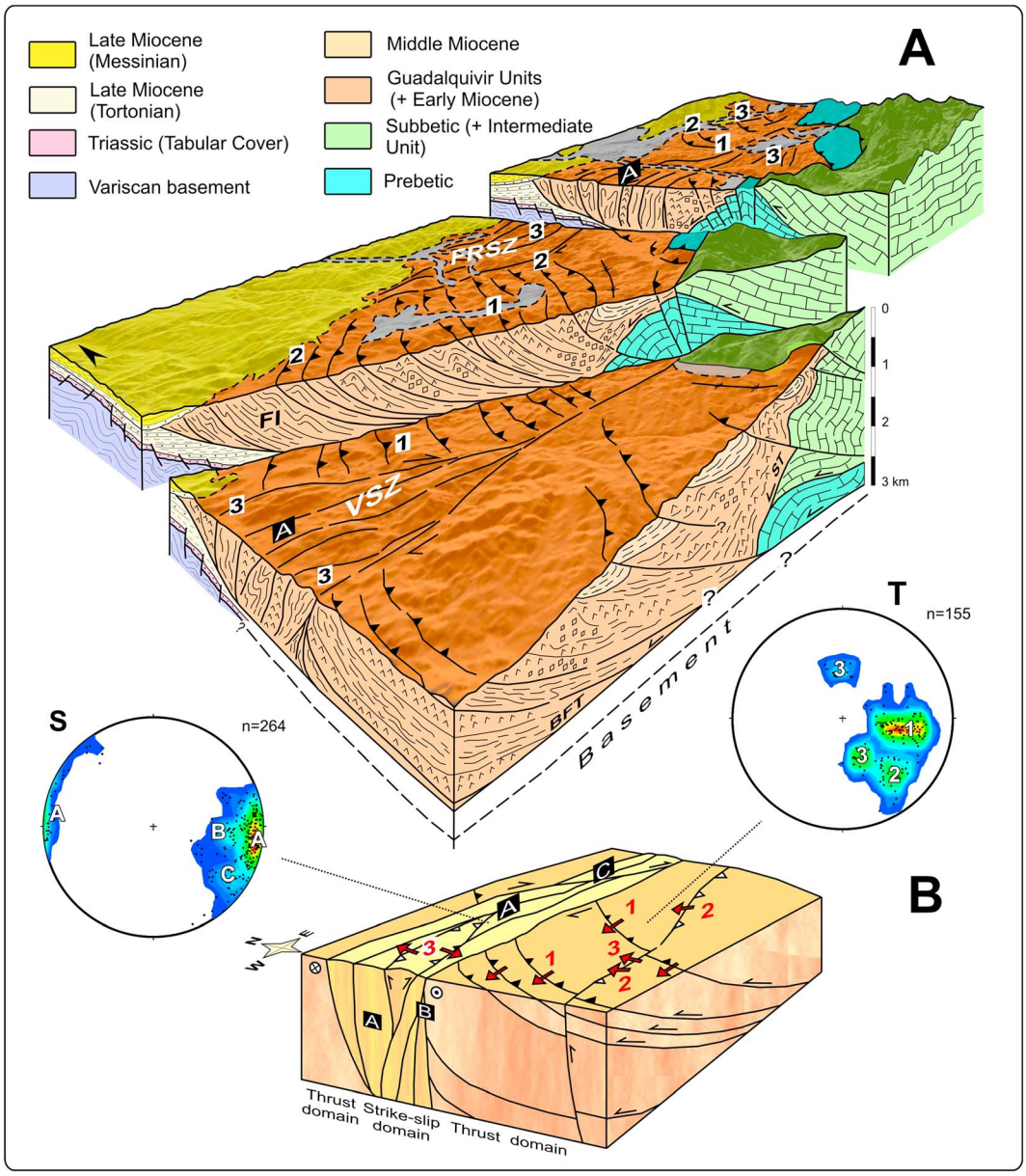

Figure 13. (a) Three-dimensional reconstruction of the Guadalquivir Accretionary Complex at the north end of the Betic Cordillera, based on field data, seismic lines, and well data. Deep of basement from *Fernàndez et al.* [1998] and *García-Castellanos et al.* [2002]. SB: Subbetic Thrust; BFT: Betic Floor Thrust. (b) Tectonic model of structures in GAC, with the stereoplots of the total thrust data (T) and strike-slip data (S). Further explanation in the text.

vector and the thrust trace, which can be interpreted as a spreading frontal thrust over a local basin. The most common situation is the dragging of the structures in the contact with the lateral shear zones (see sketch in Figure 13b). Nevertheless, strain partitioning could explain the existence of perpendicular kinematic indicators on the same structure under the same stress regime (i.e., perpendicular gypsum fibers in planes, SIB-1, and striae in scaly clays, ANV-4, Figure 4), especially in transpressional strike-slip zones with a vertical extrusion [*Martínez-Díaz*, 2002; *Jones et al.*, 2004; *Fernández and Díaz-Aspiroz*, 2009] (Figure 13b). Recent transpressional tectonics has been described near the GAC in Quaternary seismic active fault zones in the Guadiana Menor sector [*Pérez-Valera et al.*, 2012].

The isolated structural observations in the area [*Frizon De Lamotte et al.*, 1991; *Guezou et al.*, 1991] showing north vergence seem to agree with those models of the Betics and Rif that envisaged the collapse of a

thickened lithosphere in the Alborán Sea [e.g., *Platt and Vissers*, 1989; *Platt et al*., 2003] and the coeval radial development of thrust systems. Nevertheless, our observations reveal that north and south vergences are related to positive-flower structures along E-W oriented shear zones. On the other hand, variations in the direction of compression in the Betic-Rif orogen since the Neogene [e.g., *Galindo-Zaldívar et al*., 1993] could also explain orthogonal vectors but distributed along the area, not concentrated on the same shear fault systems. Therefore, the alternation of curved trust belts with transfer shear zones fits with an oblique convergence scenario. This situation is predicted by the current models of westward rollback [e.g., *Lonergan and White*, 1997] and can also explain the near east-west elongation of the Guadalquivir Basin in this sector.

6.2. Emplacement of Guadalquivir Accretionary Complex

One of the main features to be considered in the emplacement of the GAC is the predominantly Subbetic nature of the GU, which implies a large thrust of the Subbetic units overtaking the Prebetic units (Subbetic Thrust of *Guezou et al*. [1991]) at the frontal part of the orogen (Figure 13a). In the eastern Betics, the Subbetic thrust took place in the middle Miocene [*García-Hernández et al*., 1973] and corresponds to a large thrust sheet where Triassic evaporites and clay-rich, marly Cretaceous-Paleogene units comprise a tectonic unit above the décollement of the thrust sheet [*Baena and Jerez Mir*, 1982; *Hermes*, 1985]. To the west, the WNW transport of the Subbetic units is laterally accommodated by the dextral strike-slip Tíscar Fault and other dextral transpressive active zones (Collejares Fault) that constitute the northern limit of a large-scale (kilometric) transfer, dextral shear zone in the southwestern corner of the Cazorla Arc [*Platt et al*., 2003; *Pérez-Valera et al*., 2006, 2012]. This zone is already composed of mostly Triassic evaporites and highly deformed Cretaceous-Paleogene pelagic, clay-rich units [*Pérez-Valera*, 2005; *Pérez-Valera et al*., 2006]. The nature, kinematics, and deformation style of the tectonic units at the south end of the Cazorla Arc, including the gypsum tectonic fabrics, are quite similar to those in the GU. In addition, considering that the end of the Cazorla Arc constitutes the eastern boundary of the GU, this sector is the most plausible zone where the GUs outstrip the parautochthonous Prebetic units, which have a significantly thinner evaporitic sole [*Andrieux and Nebbad*, 1996] and thus a limited capacity of movement. This limited capacity has been demonstrated in an analogical experiment with the use of plastic décollements [*Luján et al*., 2003] or in orogens with ductile detachments compared to frictional detachments [*Cotton and Koyi*, 2000].

In the study area, reverse and oblique transpressive faults affect the faulting and folding of the Subbetic Thrust after its formation, as occurs in the eastern Betics [*Meijninger and Vissers*, 2007]. This subsequent deformation is responsible for the formation of the current topographic mountain front, which constitutes, in fact, an out-of-sequence mountain front in which the Prebetic isolated outcrops of the eastern Guadalquivir (Prebetic of Jaén) can be considered uplifted tectonic windows (Figure 13a). Therefore, the mountain front is retracted several kilometers from the GAC front and consequently does not represent the north end of deformation in the Betic Cordillera as described by some authors [*Roldán-García*, 1994; *Ruano et al*., 2004; *García-Tortosa et al*., 2008]. Furthermore, the age of this out-of-sequence deformation is post-Tortonian since marine sediments of this age are deformed in the Jódar-Bedmar area [*Sanz de Galdeano et al*., 2013] and Pliocene-Quaternary alluvial sediments are clearly folded and faulted throughout the mountain front [*García-Tortosa et al*., 2008], suggesting recent activity. These data contradict the inactivity of the front in this sector proposed by *Ruiz-Constán et al*. [2009]. On the contrary, the mountain front continues moving to the WNW with moderate rates, constituting a new "backstop" for the GAC.

Therefore, the Prebetic massifs display a geometry that could have influenced the observed alternating arcs and transfer zones. Points A and B in Figure 12 represent abrupt curvature points of the mountain front that correspond to irregular indenters coinciding with the start of the GAC transfer zones (FRSZ and VSZ) (Figure 12). This configuration can indicate differential deformation speeds that would have to be higher to the south to generate the dextral transfer zones. In some analogue models, an irregular indenter or different backstop velocities can cause the formation of transfer zones [*Calassou et al*., 1993; *Reiter et al*., 2011; *Ruh et al*., 2013] as well as arcuate accretionary wedges [*Zweigel*, 1998], as can also be seen in natural accretionary wedges or fold-and-thrust belts [e.g., *Coutand et al*., 2002; *Regard et al*., 2004; *Sobel et al*., 2011].

In summary, the main phase of GAC emplacement took place during the early-middle Miocene, ending in the late Miocene (Tortonian). During the emplacement, the progressive advance of the accretionary wedge is the responsible for the deformational features present of the GU, observed in the mélange units. Early and middle Miocene sediments, located over the GAC, can be considered piggyback basins deformed by the

oblique reverse and strike-slip faults due to the continuous advance of the wedge. At the same time, the direction of GAC emplacement is still WNW, with the GAC basal thrust (Betic Floor Thrust of *Guezou et al*. [1991]) also affecting autochthonous Miocene sediments of the Guadalquivir Basin (Figure 13a). The main GAC movements are postdated by calcareous sandstones and marls of Tortonian age [*Sierro et al*., 1996; *García et al*., 2014], although progressive unconformities (Figure 12), folds, and faults affecting the Tortonian and Messinian units at the Fuerte del Rey, Garcíez, and Valenzuela Shear Zones (FRSZ, GSZ, and VSZ) indicate lower to moderate tectonic activity after the main emplacement phase of the GAC, related to the out-of-sequence faults that generate the current mountain front. Late Miocene, Pliocene, and Quaternary deposits are locally faulted and folded [*García-Tortosa et al*., 2008; *Pérez-Valera et al*., 2012], and moderate seismic activity is present in the area [*Pedrera et al*., 2013; *Sánchez-Gómez et al*., 2014; *Morales et al*., 2015]. Tectonic activity in the zone has continued until the present, probably with lower rates of horizontal displacement. This recent activity must have determined the present-day elevation of the carbonate massif that configures the mountain front [*Sanz de Galdeano and Alfaro*, 2004], obliterating its original relationships with the GAC and thus hiding early tectonic processes.

6.3. Previous Hypotheses on Evaporitic Rock Emplacement

Other hypotheses attempted to explain the singularities of this key sector of the Betic Cordillera on the basis of partial or misinterpreted data. They can be grouped into two main groups (the lateral diapir and the olistostromic hypotheses) that are incorporated in some form in most geological works on the area.

6.3.1. The Olistostromic Hypothesis

The active border of a foreland basin is a typical site for the formation of olistostromes and other chaotic deposits [*Peybernès et al*., 2001; *Alonso et al*., 2006; *Codegone et al*., 2012; *Ogata et al*., 2012]. The advance of an accretionary wedge over a foreland basin produces topographic uplift that creates gravitational instability at the mountain belt front and progressive slope failure drives the emplacement of mass waste deposits, forming olistostromes [*Lucente and Pini*, 2003, 2008; *Medialdea et al*., 2004; *Smit et al*., 2010]. Classically, olistostromes are composed of a variety of reworked material constituted by different sized particles (from muddy sediments to large blocks termed olistoliths) that generally occur as chaotic monomictic/polymictic, matrix-supported breccias or megabreccias where a block-in-matrix fabric can be observed [*Abbate et al*., 1970; *Hoedemaker*, 1973; *Festa et al*., 2012, and references therein].

The regional- and cartographic-scale apparent chaotic features of the Triassic evaporites and Cretaceous-Paleogene clay-rich formations in the southern margin of the Guadalquivir Basin have been interpreted as the result of sedimentary emplacement by large-scale mass wasting from the Betic mountain front. The large amount of gypsum breccias that define outcrop-scale banding (pseudobedding) together with decametric-hectometric blocks floating in an evaporite-rich matrix could form a thick olistostrome that represents the infill of the Guadalquivir foreland basin from its active margin. This hypothesis has been proposed by *Perconig* [1960], *Roldán-García and García-Cortés* [1988], *Roldán-García* [1994], *Pérez-López and Sanz de Galdeano* [1994], and *Riaza and Martínez del Olmo* [1996]. However, although an olistostromic hypothesis seems possible in this geological context, some of the features revealed in this work cannot be explained in this way:

1. Sedimentary features (e.g., bedding, grain size organization, grain avalanching, and rock fall) and stratal disruption phenomena (slumping, intraformational breccias, and coherent or incoherent slides) typical in olistostromes [e.g., *Hoedemaker*, 1973] are absent in the Guadalquivir Units. In addition, basinal autochthonous material (e.g., turbidites and pelagic marls), breccias, or conglomerates are clearly present in the Miocene units above the GU (units I and II, Figure 3), while these materials are not present in the GU. On the contrary, the presence of massive gypsum breccias with deformational features in the evaporite-bearing units of the type I melánge can be observed in typical (salt-driven) diapirs [*De Ruig*, 1995; *Roca et al*., 1996], tectonic shaped diapirs, or sheared evaporite units along the Betic Cordillera, the last related with deformation in strike-slip contexts: Crevillente Fault [*De Smet*, 1984], Socovos Fault [*Pérez-Valera et al*., 2010], Tíscar and Collejares Faults [*Sanz de Galdeano et al*., 2006; *Pérez-Valera et al*., 2011b], Antequera zone [*Calaforra and Pulido-Bosch*, 1999], and thrust-and-folds tectonic settings [*Pedrera et al*., 2012]. Also, the presence in the subsurface of halite masses in the GU (see the saltworks and saline springs in Figure 2) reveals that salt tectonics processes have played an important role in the deformational history of GU since their emplacement as diapirs or allocthonous salt sheets in the

passive margin stage of the South Iberian Palaeomargin [*Flinch*, 2003]. Moreover, evaporites cannot constitute a reliable sedimentary olistostrome matrix due to their limited properties to be reworked or resedimented (e.g., dissolution processes). Only salt glaciers could mass transport evaporites downslope when diapirs or allocthonous salt sheets extrude in a submarine/subaerial surface, but the internal fabric, structures, and deformation mechanism are very different from that produced by sedimentary processes and more related with salt tectonics [*Wenkert*, 1979; *Wu et al*., 1990; *Talbot and Pohjola*, 2009].

2. In an olistostrome, the source area that supplies the sediment into the foreland basin is well known and, in most cases, the feed areas have been reconstructed in detail [*Alonso et al*., 2006; *Lucente and Pini*, 2008]. In the study area, the hypothetical source area of the olistostrome would be the Betic mountain front, which is formed by carbonates of Subbetic and Prebetic units (Figures 2, 10, and 13). A detailed examination of the GU shows that there is no correlation between the Betic mountain front source area and the composition of the GU (formed of marl and clay-rich units of Subbetic origin and mélange-type units). Specifically, neither Triassic (70% of the GU) nor Cretaceous-Paleogene Subbetic material crops out anywhere in this sector of the Betic mountain front. Nevertheless, clasts from several Jurassic units of the Subbetic Domain are present in the bioclastic carbonate breccias of Unit I (early Miocene, Figure 3) and in the clastics deposits of Unit II (middle Miocene, Figure 3), thus indicating that the source area for these units does correspond to this part of the mountain front. Moreover, the dipping of the supposed bedding of the olistostromic deposits would have to be to the northwest, toward the foreland basin. Instead, the tectonic banding observed in the GU dips to the southeast (Figure 13), opposite to the Betic mountain front and coherent with the expected thrusting vergence in an accretionary system, as also suggested by the seismic lines (Figure 11) and the field data (Figure 12).
3. Finally, in the olistostromic hypothesis, the age of olistostrome emplacement ranges between the Late Langhian-Early Serravalian [*Roldán-García*, 1994] and Late Tortonian [*Riaza and Martínez del Olmo*, 1996]. The association of middle Miocene ages through planktonic microfossils for the brecciated material of GU is the most consistent argument for the gravitational emplacement of GU in the Guadalquivir Basin [*Roldán-García*, 1994; *Rodríguez-Fernández et al*., 2013]. Nevertheless, after numerous attempts of dating the evaporite-clay matrix (mélange type I) no microfossils were found. On the other hand, materials included in the mélange type II show planktonic microfossils with reliable biostratigraphic ages consistent with their derived Cretaceous-Paleogene units. Furthermore, microfossils data from the Miocene units reveal the existence of two syntectonics units of latest Oligocene to middle Miocene age (Units I and II, Figure 3) and one posttectonic unit of late Miocene age (Unit III, Figure 3) [*Sierro et al*., 1996; *García et al*., 2014]. These Miocene units were disrupted, deformed, folded, and faulted during the tectonic emplacement of the accretionary body. In fact, Miocene units I and II are actually part of the GAC in its frontal end usually as small tectonic slices (e.g., frontal imbricates, Figure 13) or remain as deformed piggyback basins over the GU (e.g., Almenara and Las Salinas basins, Figures 7 and 8). In this stratigraphic and tectonic context, the emplacement of the GU as a huge gravitational olistostromic deposit at the same age as Miocene units show several problems. Aspects as accommodation space, basin geometry, stratigraphic organization, facies evolution, and, especially, correlations of the supposed olistostromes with their coetaneous units are difficult to explain if the gravitational model is assumed. Therefore, with the data present in this paper, the GU cannot be considered part of the sedimentary infill of the Guadalquivir Basin as the olistostromic hypothesis suggests.

6.3.2. The Lateral Diapir Hypothesis

The profuse development of salt structures (diapirs, allochthonous sheets, canopies, etc.) in the passive stage of a continental margin can generate a large amount of brecciated material due to the plastic migration and dissolution of salt, resulting in thick evaporitic breccias (halite and gypsum/anhydrite) with shales having decametric blocks of siliciclastic and carbonate rocks forming an insoluble residuum or caprock [*Trusheim*, 1960; *Friedman*, 1997]. If this evaporitic brecciated material is deformed during contraction and incorporated into a fold-and-thrust belt, its weakness and ductility are suitable for forming detachment horizons [*Davis and Engelder*, 1985]; *Sans*, 2003], with a tectonic fabric overlapping the dissolution breccias [*Malavieille and Ritz*, 1989; *Rouchy et al*., 1993]. Moreover, salt tectonics can still work after or during the compressive processes, that is, generating new tectonically controlled diapirs while salt migration pathways remain open [e.g., *Calaforra and Pulido-Bosch*, 1999; *Pérez-Valera et al*., 2010]. Consequently, evaporites have been described in a large variety of fold-and-thrust belts, performing a pivotal role in the structural styles [*Chen et al*., 2004; *Moretti et al*., 2010; *Trudgill*, 2011; *Pedrera et al*., 2012].

Based on the large amount of evaporite-rich breccias and on geophysical and field data, *Berástegui et al*. [1998] proposed and modeled a northward lateral diapiric emplacement of Triassic evaporites in the southern Guadalquivir Basin, as a chaotic unit with frontal imbricates, strongly arguing the olistostrome hypothesis. However, the diapir hypothesis by *Berástegui et al*. [1998] could also be discussed on the basis of data in this work: (1) Structural and kinematic data provided in GU gypsum-bearing rocks are not consistent with a lateral diapir emplaced by a northward expulsion of evaporites from the south. The origin of the diapir below the Intermediate Unit (part of the Subbetic Zone) is speculative; thus, the 40 km shortening proposed from structural cross sections is considerably less than can be estimated, considering that the true tectonic transport is to the WNW. (2) The chaotic unit corresponds, in fact, to a well-structured WNW vergent thrust slice system with dextral lateral subvertical fault zones in which limestone blocks, interpreted as randomly oriented blocks in the caprock of the supposed diapir, constitute remnants of the Zamoranos Formation (Late Triassic), largely boudinaged and dismembered in a plastic-viscous evaporite-rich mélange. Therefore, although salt tectonic processes can be present in the GU, their role may be considered only local versus the overall tectonic processes involved in the formation of the accretionary complex.

7. Conclusions

The structural and mapping analysis of an area outside the present-day Betic mountain front at the eastern end of the Guadalquivir Basin reveals a well-organized accretionary complex composed mainly of Triassic evaporites and other clay-bearing sheets of Cretaceous, Paleogene, and Neogene age together with mélange-like bodies forming the Guadalquivir Units (GUs). This accretionary complex has been named the Guadalquivir Accretionary Complex (GAC) and displays a coherent kinematic setting provided by well-developed scaly fabrics in clay-rich sediments and gypsum S- and L-tectonites, which include lineations such as rod or sheath folds distinctive of ductile deformation. The observations are in agreement with an accretionary system formed at the north end of the Betic Cordillera from the early Miocene to the Tortonian but disagree with the sedimentary (olistostromic) and lateral diapir interpretations proposed by previous authors.

The GAC structure consists of alternating domains of N-S to NNE-SSW arc-shaped systems separated by dextral, transfer, or wrench zones. The transfer and thrust kinematics are consistent and indicate a westward motion (top-to 290°) of the southeastern parts of the system. However, at the same time, limited N-S shortening is evidenced mainly by folding and flower structures along the transfer zones. The pervasive and systematic west directed structures of the GAC fold-and-thrust trends are better suited with the tectonic models that imply the westward retreat of a lithospheric slab resulting in oblique convergence between the Alborán Domain and the South Iberian Paleomargin. Other slab retreat directions or tectonic models, such as lithospheric delamination, cannot explain the consistent kinematic of the GAC showed in this study.

To understand the emplacement of the GAC and the apparent mismatch that these units pose with respect to the rest of the Betics, it should be considered that (1) the abundance of Triassic salt and other incompetent evaporites in the GAC, and their migration in the passive margin stage, allows them to form a very low angle thrust wedge that considerably surpassed the carbonate massif front during the main collision stage (early-middle Miocene) and (2) the late Miocene to Quaternary topographic rise of the carbonate massifs masked the pristine structure, relegating evaporite-bearing GAC units to relatively depressed areas. Nevertheless, the GAC should be considered a genuine toe of the Betic thrust wedge and as such reflects in its brittle and ductile structures the Betic oblique collision in a segment nearly parallel to the direction of movement. This feature makes the eastern GAC an exceptional place to understand strain partitioning in a highly oblique setting.

Acknowledgments

The data for this paper are available by contacting the corresponding author. Original seismic lines used in this paper can be obtained from the database of the Spanish Geological Survey (www.igme.es). This study was supported by research projects CGL2012-33281 and CGL2013-46368-P (Secretaría de Estado de I+D+I, Spain), CeacTierra-Universidad de Jaén, RNM-0451 (Junta de Andalucía), and by the Junta de Andalucía Research Groups RNM 208, 325, and 370. We are grateful to Francisco Serrano for the micropaleontological determinations. Comments by David Iacopini, Giancarlo Molli, and the Associate Editor have significantly improved this paper. We also thank A. Azor for the suggestions on a previous version of this manuscript and Christine Laurin for revising the English.

References

Abbate, E., V. Bortolotti, and P. Passerini (1970), Olistostromes and olistoliths, *Sediment. Geol.*, *4*(3–4), 521–557, doi:10.1016/0037-0738(70)90022-9.

Alonso, J. L., A. Marcos, and A. Suárez (2006), Structure and organization of the Porma Mélange: Progressive denudation of a submarine nappe toe by gravitational collapse, *Am. J. Sci.*, *306*(1), 32–65, doi:10.2475/ajs.306.1.32.

Andrieux, J., and F. Nebbad (1996), El prisma orogénico prebético, *Geogaceta*, *20*(4), 810–812.

Andrieux, J., J. M. Fontbote, and M. Mattauer (1971), Sur un modele explicatif de l'arc de Gibraltar, *Earth Planet. Sci. Lett.*, *12*(2), 191–198, doi:10.1016/0012-821X(71)90077-X.

Baena, J., and L. Jerez Mir (1982), *Síntesis para un ensayo paleogeográfico entre la Meseta y la Zona Bética (s. str.)*, pp. 1–256, Colección Informe, IGME, Madrid.

Bahroudi, A., and H. Koyi (2003), Effect of spatial distribution of Hormuz salt on deformation style in the Zagros fold and thrust belt: An analogue modelling approach, *J. Geol. Soc. London*, *160*(5), 719–733, doi:10.1144/0016-764902-135.

Balanyá, J. C., and V. García-Dueñas (1987), Les directions structurales dans le Domaine d'Alborán de part et d'autre du Détroit de Gibraltar, *Comptes rendus de l'Académie des sciences*. Série 2, Mécanique, Physique, Chimie, Sciences de l'univers, *Sci. Terre*, *304*(15), 929–932.

Balanyá, J. C., V. García-Dueñas, J. M. Azañón, and M. Sánchez-Gómez (1997), Alternating contractional and extensional events in the Alpujarride nappes of the Alboran Domain (Betics, Gibraltar Arc), *Tectonics*, *16*(2), 226–238, doi:10.1029/96TC03871.

Balanyá, J. C., V. García-Dueñas, J. M. Azañon, and M. Sánchez-Gómez (1998), Comment on "alternating contractional and extensional events in the Alpujarride nappes of the Alboran Domain (Betics, Gibraltar arc)"—Reply, *Tectonics*, *17*, 977–981.

Balanyá, J. C., A. Crespo-Blanc, M. Díaz-Aspiroz, I. Expósito, and M. Luján (2007), Structural trend line pattern and strain partitioning around the Gibraltar Arc accretionary wedge: Insights as to the mode of orogenic arc building, *Tectonics*, *26*, TC2005, doi:10.1029/2005TC001932.

Barcos, L., J. C. Balanyá, M. Díaz-Azpiroz, I. Expósito, and A. Jiménez-Bonilla (2015), Kinematics of the Torcal Shear Zone: Transpressional tectonics in a salient-recess transition at the northern Gibraltar Arc, *Tectonophysics*, *663*, 62–77, doi:10.1016/j.tecto.2015.05.002.

Berástegui, X., C. J. Banks, C. Puig, C. Taberner, D. Waltham, and M. Fernàndez (1998), Lateral diapiric emplacement of Triassic evaporites at the southern margin of the Guadalquivir Basin, Spain, *Geol. Soc. London Spec. Publ.*, *134*(1), 49–68, doi:10.1144/GSL.SP.1998.134.01.04.

Bezada, M. J., E. D. Humphreys, D. R. Toomey, M. Harnafi, J. M. Dávila, and J. Gallart (2013), Evidence for slab rollback in westernmost Mediterranean from improved upper mantle imaging, *Earth Planet. Sci. Lett.*, *368*, 51–60, doi:10.1016/j.epsl.2013.02.024.

Blankenship, C. L. (1992), Structure and palaeogeography of the External Betic Cordillera, southern Spain, *Mar. Pet. Geol.*, *9*(3), 256–264, doi:10.1016/0264-8172(92)90074-O.

Blumenthal, M. (1927), Versuch einer tektonischen Gliederug der betischen Cordilleren von Central, und Sud-West Andalusien, *Eclogae Geol. Helv.*, *20*, 487–592.

Bokelmann, G., E. Maufroy, L. Buontempo, J. Morales, and G. Barruol (2011), Testing oceanic subduction and convective removal models for the Gibraltar arc: Seismological constraints from dispersion and anisotropy, *Tectonophysics*, *502*(1–2), 28–37, doi:10.1016/j.tecto.2010.08.004.

Booth-Rea, G., J. M. Azañón, J. M. Martínez-Martínez, O. Vidal, and V. García-Dueñas (2005), Contrasting structural and P-T evolution of tectonic units in the southeastern Betics: Key for understanding the exhumation of the Alboran Domain HP/LT crustal rocks (western Mediterranean), *Tectonics*, *24*, TC2009, doi:10.1029/2004TC001640.

Boutelier, D., and A. Cruden (2013), Slab rollback rate and trench curvature controlled by arc deformation, *Geology*, *41*(8), 911–914, doi:10.1130/G34338.1.

Burg, J.-P., D. Bernoulli, J. Smit, A. Dolati, and A. Bahroudi (2008), A giant catastrophic mud-and-debris flow in the Miocene Makran, *Terra Nov.*, *20*(3), 188–193, doi:10.1111/j.1365-3121.2008.00804.x.

Calaforra, J. M., and A. Pulido-Bosch (1999), Gypsum karst features as evidence of diapiric processes in the Betic Cordillera, Southern Spain, *Geomorphology*, *29*(3–4), 251–264, doi:10.1016/S0169-555X(99)00019-7.

Calassou, S., C. Larroque, and J. Malavieille (1993), Transfer zones of deformation in thrust wedges: An experimental study, *Tectonophysics*, *221*(3–4), 325–344, doi:10.1016/0040-1951(93)90165-G.

Calvert, A., E. Sandvol, D. Seber, M. Barazangi, S. Roecker, T. Mourabit, F. Vidal, G. Alguacil, and N. Jabour (2000), Geodynamic evolution of the lithosphere and upper mantle beneath the Alboran region of the western Mediterranean: Constraints from travel time tomography, *J. Geophys. Res.*, *105*(B5), 10871–10898, doi:10.1029/2000JB900024.

Candansayar, M. E. (2008), Two-dimensional individual and joint inversion of three- and four-electrode array dc resistivity data, *J. Geophys. Eng.*, *5*(3), 290, doi:10.1088/1742-2132/5/3/005.

Castelló Montorí, R., F. Orviz Castro, and R. Pignatelli García (1972), *Mapa Geológico de España a escala 1:50000. Mapa y Memoria de la Hoja 924 (Bujalance)*, pp. 1–22, IGME, Madrid.

Chen, S., L. Tang, Z. Jin, C. Jia, and X. Pi (2004), Thrust and fold tectonics and the role of evaporites in deformation in the Western Kuqa Foreland of Tarim Basin, Northwest China, *Mar. Pet. Geol.*, *21*(8), 1027–1042, doi:10.1016/j.marpetgeo.2004.01.008.

Chiang, C. S., H. S. Yu, and Y. W. Chou (2004), Characteristics of the wedge-top depozone of the southern Taiwan foreland basin system, *Basin Res.*, *16*(1), 65–78, doi:10.1111/j.1365-2117.2004.00222.x.

Cladouhos, T. T. (1999), A kinematic model for deformation within brittle shear zones, *J. Struct. Geol.*, *21*(4), 437–448, doi:10.1016/S0191-8141(98)00124-2.

Codegone, G., A. Festa, Y. Dilek, and G. A. Pini (2012), Small-scale polygenetic mélanges in the Ligurian accretionary complex, Northern Apennines, Italy, and the role of shale diapirism in superposed mélange evolution in orogenic belts, *Tectonophysics*, *568–569*(0), 170–184, doi:10.1016/j.tecto.2012.02.003.

Comas, M. C., J. P. Platt, J. I. Soto, and A. B. Watts (1999), The origin and tectonic history of the Alboran Basin: Insights from Leg 161 results, *Proc. Ocean Drill. Program Sci. Results*, *161*, 555–580.

Copley, A. (2012), The formation of mountain range curvature by gravitational spreading, *Earth Planet. Sci. Lett.*, *351–352*, 208–214, doi:10.1016/j.epsl.2012.07.036.

Costa, E., and B. C. Vendeville (2002), Experimental insights on the geometry and kinematics of fold-and-thrust belts above weak, viscous evaporitic décollement, *J. Struct. Geol.*, *24*(11), 1729–1739, doi:10.1016/S0191-8141(01)00169-9.

Cotton, J. T., and H. A. Koyi (2000), Modeling of thrust fronts above ductile and frictional detachments: Application to structures in the Salt Range and Potwar Plateau, Pakistan, *Geol. Soc. Am. Bull.*, *112*(3), 351–363, doi:10.1130/0016-7606(2000)112<351:MOTFAD>2.0.CO;2.

Coutand, I., M. R. Strecker, J. R. Arrowsmith, G. Hilley, R. C. Thiede, A. Korjenkov, and M. Omuraliev (2002), Late Cenozoic tectonic development of the intramontane Alai Valley, (Pamir-Tien Shan region, central Asia): An example of intracontinental deformation due to the indo-Eurasia collision, *Tectonics*, *21*(6), 1053, doi:10.1029/2002TC001358.

Cowan, D. S. (1985), Structural styles in Mesozoic and Cenozoic mélanges in the western Cordillera of North America, *Geol. Soc. Am. Bull.*, *96*(4), 451–462.

Coward, M. P., M. De Donatis, S. Mazzoli, W. Paltrinieri, and F. C. Wezel (1999), Frontal part of the northern Apennines fold and thrust belt in the Romagna-Marche area (Italy): Shallow and deep structural styles, *Tectonics*, *18*(3), 559–574, doi:10.1029/1999TC900003.

Crespo-Blanc, A. (2007), Superimposed folding and oblique structures in the palaeomargin-derived units of the Central Betics (SW Spain), *J. Geol. Soc. London*, *164*(3), 621–636, doi:10.1144/0016-76492006-084.

Crespo-Blanc, A., and J. Campos (2001), Structure and kinematics of the South Iberian paleomargin and its relationship with the Flysch Trough units: Extensional tectonics within the Gibraltar Arc fold-and-thrust belt (western Betics), *J. Struct. Geol.*, *23*(10), 1615–1630, doi:10.1016/S0191-8141(01)00012-8.

Crespo-Blanc, A., and D. F. de Lamotte (2006), Structural evolution of the external zones derived from the Flysch trough and the South Iberian and Maghrebian paleomargins around the Gibraltar arc: A comparative study, *Bull. Soc. Geol. Fr.*, *177*(5), 267–282, doi:10.2113/gssgfbull.177.5.267.

Davis, D., J. Suppe, and F. A. Dahlen (1983), Mechanics of fold-and- thrust belts and accretionary wedges, *J. Geophys. Res.*, *88*(B2), 1153–1172.

Davis, D. M., and T. Engelder (1985), The role of salt in fold-and-thrust belts, *Tectonophysics*, *119*(1–4), 67–88, doi:10.1016/0040-1951(85)90033-2.

De Paola, N., C. Collettini, D. R. Faulkner, and F. Trippetta (2008), Fault zone architecture and deformation processes within evaporitic rocks in the upper crust, *Tectonics*, *27*, TC4017, doi:10.1029/2007TC002230.

De Ruig, M. J. (1995), Extensional diapirism in the eastern Prebetic foldbelt, southeastern Spain, in *Salt Tectonics: A Global Perspective*, *AAPG Memoir 65*, edited by M. P. A. Jackson, D. G. Roberts, and S. Snelson, pp. 353–367, American Association of Petroleum Geologist, Tulsa, Okla.

De Smet, M. E. M. (1984), Wrenching in the external zone of the Betic Cordilleras, southern Spain, *Tectonophysics*, *107*(1–2), 57–79.

Del Ben, A., C. Barnaba, and A. Taboga (2008), Strike-slip systems as the main tectonic features in the Plio-Quaternary kinematics of the Calabrian Arc, *Mar. Geophys. Res.*, *29*(1), 1–12, doi:10.1007/s11001-007-9041-6.

Docherty, C., and E. Banda (1995), Evidence for the eastward migration of the Alboran Sea based on regional subsidence analysis: A case for basin formation by delamination of the subcrustal lithosphere?, *Tectonics*, *14*(4), 804–818, doi:10.1029/95TC00501.

Duarte, J. C., F. M. Rosas, P. Terrinha, M. A. Gutscher, J. Malavieille, S. Silva, and L. Matias (2011), *Mar. Geol.*, *289*(1–4), 135–149, doi:10.1016/j.margeo.2011.09.014.

Duggen, S., K. Hoernle, P. Van den Bogaard, and D. Garbe-Schonberg (2005), Post-collisional transition from subduction- to intraplate-type magmatism in the westernmost Mediterranean: Evidence for continental-edge delamination of subcontinental lithosphere, *J. Petrol.*, *46*, 1155–1201.

Duggen, S., K. Hoernle, P. van den Bogaard, and C. Harris (2004), Magmatic evolution of the Alboran region: The role of subduction in forming the western Mediterranean and causing the Messinian Salinity Crisis, *Earth Planet. Sci. Lett.*, *218*(1–2), 91–108, doi:10.1016/S0012-821X(03)00632-0.

Duggen, S., K. Hoernle, A. Klügel, J. Geldmacher, M. Thirlwall, F. Hauff, D. Lowry, and N. Oates (2008), Geochemical zonation of the Miocene Alborán Basin volcanism (westernmost Mediterranean): Geodynamic implications, *Contrib. Mineral. Petrol.*, *156*(5), 577–593, doi:10.1007/s00410-008-0302-4.

Durand-Delga, M., P. Rossi, P. Olivier, and D. Puglisi (2000), Situation structurale et nature ophiolitique de roches basiques jurassiques associées aux flyschs maghrébins du Rif (Maroc) et de Sicile (Italie), *C. R. Acad. Sci., Ser. IIA Earth Planet. Sci.*, *331*(1), 29–38, doi:10.1016/S1251-8050(00)01378-1.

Egydio-Silva, M., A. Vauchez, M. I. B. Raposo, J. Bascou, and A. Uhlein (2005), Deformation regime variations in an arcuate transpressional orogen (Ribeira belt, SE Brazil) imaged by anisotropy of magnetic susceptibility in granulites, *J. Struct. Geol.*, *27*(10), 1750–1764, doi:10.1016/j.jsg.2005.06.001.

Faccenna, C., C. Piromallo, A. Crespo-Blanc, L. Jolivet, and F. Rossetti (2004), Lateral slab deformation and the origin of the western Mediterranean arcs, *Tectonics*, *23*, TC1012, doi:10.1029/2002TC001488.

Fadil, A., P. Vernant, S. McClusky, R. Reilinger, F. Gomez, D. B. Sari, T. Mourabit, K. Feigl, and M. Barazangi (2006), Active tectonics of the western Mediterranean: Geodetic evidence for rollback of a delaminated subcontinental lithospheric slab beneath the Rif Mountains, Morocco, *Geology*, *34*(7), 529–532, doi:10.1130/G22291.1.

Fernández, C., and M. Díaz-Aspiroz (2009), Triclinic transpression zones with inclined extrusion, *J. Struct. Geol.*, *31*(10), 1255–1269, doi:10.1016/j.jsg.2009.07.001.

Fernández, J., and C. Dabrio (1985), Fluvial architecture of the buntsandstein-facies redbeds in the Middle to Upper Triassic (Ladinian-Norian) of the southeastern edge of the Iberian Meseta (Southern Spain), in *Aspects of Fluvial Sedimentation in the Lower Triassic Buntsandstein of Europe*, vol. 4, edited by D. Mader, pp. 411–435, Springer-Verlag, Berlin/Heidelberg.

Fernàndez, M., X. Berástegui, C. Puig, D. García-Castellanos, M. J. Jurado, M. Torné, and C. Banks (1998), Geophysical and geological constraints on the evolution of the Guadalquivir foreland basin, Spain, *Geol. Soc. London Spec. Publ.*, *134*(1), 29–48, doi:10.1144/GSL.SP.1998.134.01.03.

Festa, A., G. A. Pini, Y. Dilek, and G. Codegone (2010), Mélanges and mélange-forming processes: A historical overview and new concepts, *Int. Geol. Rev.*, *52*(10–12), 1040–1105, doi:10.1080/00206810903557704.

Festa, A., Y. Dilek, G. A. Pini, G. Codegone, and K. Ogata (2012), Mechanisms and processes of stratal disruption and mixing in the development of mélanges and broken formations: Redefining and classifying mélanges, *Tectonophysics*, *568–569*, 7–24.

Festa, A., K. Ogata, G. A. Pini, Y. Dilek, and G. Codegone (2015), Late Oligocene-early Miocene olistostromes (sedimentary mélanges) as tectono-stratigraphic constraints to the geodynamic evolution of the exhumed Ligurian accretionary complex (Northern Apennines, NW Italy), *Int. Geol. Rev.*, *57*(5–8), 540–562, doi:10.1080/00206814.2014.931260.

Flinch, J. F. (1996), Accretion and extensional collapse of the external Western Rif (Northern Morocco), *Mémoires du Muséum national d'histoire naturelle*, *170*, 61–85.

Flinch, J. F. (2003), A cretaceous allochthonous evaporitic province within the Betic-Maghrebian Domain: Comparison with the present-day Gulf of Mexico, in extended abstract, International Conference AAPG.

Flinch, J. F., A. W. Bally, and S. Wu (1996), Emplacement of a passive-margin evaporitic allochthon in the Betic Cordillera of Spain, *Geology*, *24*(1), 67–70, doi:10.1130/0091-7613(1996)024<0067:EOAPME>2.3.CO;2.

Friedman, G. (1997), Dissolution-collapse breccias and paleokarst resulting from dissolution of evaporite rocks, especially sulfates, *Carbonates Evaporites*, *12*(1), 53–63, doi:10.1007/BF03175802.

Frizon De Lamotte, D., J. Andrieux, and J. C. Guezou (1991), Kinematics of the Neogene thrusting in the Betic-Rif orocline: Discussion of geodynamic models, *Bull. Soc. Geol. Fr.*, *162*(4), 611–626.

Galindo-Zaldívar, J., F. González-Lodeiro, and A. Jabaloy (1993), Stress and palaeostress in the Betic-Rif cordilleras (Miocene to the present), *Tectonophysics*, *227*(1–4), 105–126, doi:10.1016/0040-1951(93)90090-7.

Galindo-Zaldívar, J., P. Ruano, A. Jabaloy, and M. López-Chicano (2000), Kinematics of faults between Subbetic Units during the Miocene (central sector of the Betic Cordillera), *C. R. Acad. Sci. Ser., IIA Earth Planet. Sci.*, *331*(12), 811–816, doi:10.1016/S1251-8050(00)01484-1.

Galindo-Zaldivar, J., A. J. Gil, C. Sanz de Galdeano, M. C. Lacy, J. A. García-Armenteros, P. Ruano, A. M. Ruiz, M. Martínez-Martos, and P. Alfaro (2015), Active shallow extension in central and eastern Betic Cordillera from CGPS data, *Tectonophysics*, *663*, 290–301, doi:10.1016/j.tecto.2015.08.035.

García-Castellanos, D. (2002), Interplay between lithospheric flexure and river transport in foreland basins, *Basin Res.*, *14*(2), 89–104, doi:10.1046/j.1365-2117.2002.00174.x.

García-Castellanos, D., and A. Villaseñor (2011), Messinian salinity crisis regulated by competing tectonics and erosion at the Gibraltar arc, *Nature*, *480*(7377), 359–363, doi:10.1038/nature10651.
García-Castellanos, D., M. Fernàndez, and M. Torne (2002), Modeling the evolution of the Guadalquivir foreland basin (southern Spain), *Tectonics*, *21*(3), 1018, doi:10.1029/2001TC001339.
García-Dueñas, V., J. C. Balanyá, and J. M. Martínez-Martínez (1992), Miocene extensional detachments in the outcropping basement of the northern Alboran Basin (Betics) and their tectonic implications, *Geo-Mar. Lett.*, *12*(2–3), 88–95, doi:10.1007/BF02084917.
García García, F., H. A. Corbí Sevila, D. A. García Ramos, J. M. Soria Mingorance, J. E. Tent Maclús, and C. Viseras Alarcón (2014), El sector nororiental de la Cuenca de Antepaís del Guadalquivir (Cordillera Bética, Mioceno Superior): Estratigrafía, cronología y evolución sedimentaria, *Rev. Soc. Geol. Esp.*, *27*, 187–204.
García-Hernández, M., A. C. López-Garrido, and A. Pulido-Bosch (1973), Observaciones sobre el contacto Subbético-Prebético en el sector de Nerpio, *Cuad. Geol. Univ. Granada*, *4*, 77–91.
García-Hernández, M., A. C. López-Garrido, P. Rivas, C. Sanz de Galdeano, and J. A. Vera (1980), Mesozoic palaeogeographic evolution of the external zones of the Betic Cordillera, *Geologie en Mijnbouw*, *59*(2), 155–168.
García-Rosell, L. (1973), Estudio geológico de la transversal Úbeda-Huelma y sectores adyacentes (Cordilleras Béticas, provincia de Jaén), PhD thesis, Departamento de Estratigrafía y Paleontología, Universidad de Granada, Spain.
García-Tortosa, F. J., C. Sanz de Galdeano, M. Sánchez-Gómez, and P. Alfaro (2008), Tectónica reciente en el frente de Cabalgamiento Bético. Las deformaciones de Jimena y Bedmar (Jaén), *Geogaceta*, *44*, 59–62.
Ghiglione, M. C., and E. O. Cristallini (2007), Have the southernmost Andes been curved since Late Cretaceous time? An analog test for the Patagonian Orocline, *Geology*, *35*(1), 13–16, doi:10.1130/G22770A.1.
Giaconia, F., G. Booth-Rea, J. M. Martínez-Martínez, J. M. Azañõn, F. Storti, and A. Artoni (2014), Heterogeneous extension and the role of transfer faults in the development of the southeastern Betic basins (SE Spain), *Tectonics*, *33*, 2467–2489, doi:10.1002/2014TC003681.
Guezou, J. C., D. Frizon De Lamotte, M. Coulon, and J. L. Morel (1991), Structure and kinematics of the Prebetic nappe complex (southern Spain): Definition of a "Betic Floor Thrust" and implications in the Betic-Rif orocline, *Annales Tectonicae*, *5*(1), 32–48.
Gutscher, M. A., S. Dominguez, G. K. Westbrook, and P. Leroy (2009), Deep structure, recent deformation and analog modeling of the Gulf of Cadiz accretionary wedge: Implications for the 1755 Lisbon earthquake, *Tectonophysics*, *475*(1), 85–97, doi:10.1016/j.tecto.2008.11.031.
Gutscher, M. A., et al. (2012), The Gibraltar subduction: A decade of new geophysical data, *Tectonophysics*, *574–575*, 72–91, doi:10.1016/j.tecto.2012.08.038.
Harding, T. P., R. C. Vierbuchen, and N. Christie-Blick (1985), Structural styles, plate tectonic settings, and hydrocarbon traps of divergent (transtensional) wrench faults, in *Strike Slip Deformation, Basin Formation, and Sedimentation*, edited by K. T. Biddle and N. Christie-Blick, pp. 51–77, Soc. Econ. Paleont. Mineral. Spec. Publ., Okla.
Harris, R. A., R. K. Sawyer, and M. G. Audley-Charles (1998), Collisional mélange develop- ment: Geologic association of active mélange-forming processes with exhumed mélange facies in the western Banda orogen, Indonesia, *Tectonics*, *17*(3), 458–479.
Hermes, J. J. (1985), Algunos aspectos de la estructura de la Zona Subbética (Cordilleras Béticas. España meridional), *Estud. Geol.*, *41*(3–4), 157–176, doi:10.3989/egeol.85413-4709.
Hodges, M., and M. S. Miller (2015), Mantle flow at the highly arcuate northeast corner of the Lesser Antilles subduction zone: Constraints from shear-wave splitting analyses, *Lithosphere*, *7*(5), 579–587, doi:10.1130/L440.1.
Hoedemaker, P. J. (1973), Olisthostromes and other delapsional deposits, and their occurrence in the region of Moratalla (Prov. of Murcia, Spain), *Scr. Geol.*, *19*, 1–207.
Huyghe, P., J. Mugnier, R. Griboulard, Y. Deniaud, E. Gonthier, and J. Faugeres (1999), Review of the tectonic controls and sedimentary patterns in late neogene piggyback basins on the Barbados Ridge Complex, in *Sedimentary Basins of the World*, vol. 4, edited by P. Mann, pp. 369–388, Elsevier, Amsterdam.
Jaumé, S. C., and R. J. Lillie (1988), Mechanics of the Salt Range-Potwar Plateau, Pakistan: A fold-and-thrust belt underlain by evaporites, *Tectonics*, *7*(1), 57–71, doi:10.1029/TC007i001p00057.
Jones, R. R., R. E. Holdsworth, P. Clegg, K. McCaffrey, and E. Tavarnelli (2004), Inclined transpression, *J. Struct. Geol.*, *26*(8), 1531–1548, doi:10.1016/j.jsg.2004.01.004.
Jordan, P. G. (1991), Development of asymmetric shale pull-aparts in evaporite shear zones, *J. Struct. Geol.*, *13*(4), 399–409, doi:10.1016/0191-8141(91)90013-9.
Krzywiec, P., and J. Vergés (2007), Role of the Foredeep Evaporites in wedge tectonics and formation of triangle zones: Comparison of the Carpathian and Pyrenean thrust fronts, in *Thrust Belts and Foreland Basins: From Fold Kinematics to Hydrocarbon Systems*, edited by O. Lacombe et al., pp. 385–396, Springer, Berlin, Heidelberg.
Kulm, L. D., and E. Suess (1990), Relationship between carbonate deposits and fluid venting: Oregon accretionary prism, *J. Geophys. Res.*, *95*(B6), 8899–8915, doi:10.1029/JB095iB06p08899.
Lanaja, J. M. (1987), *Contribución de la Exploración Petrolífera al Conocimiento de la Geología de España*, pp. 1–465, IGME, Madrid.
Leblanc, D. (1990), Tectonic adaptation of the external zones around the curved core of an orogen: The Gibraltar Arc, *J. Struct. Geol.*, *12*(8), 1013–1018, doi:10.1016/0191-8141(90)90097-I.
Letouzey, J., B. Colleta, R. Vially, and J. C. Chermette (1995), Evolution of salt-related structures in compressional settings, in *Salt Tectonics: A Global Perspective*, *AAPG Memoir*, *65*, edited by M. P. A. Jackson et al., pp. 41–60, American Association of Petroleum Geologist, Tulsa, Okla.
Lonergan, L., and N. White (1997), Origin of the Betic-Rif mountain belt, *Tectonics*, *16*(3), 504–522, doi:10.1029/96TC03937.
Lucente, C. C., and G. A. Pini (2003), Anatomy and emplacement mechanism of a large submarine slide within a Miocene foredeep in the northern Apennines, Italy: A field perspective, *Am. J. Sci.*, *303*(7), 565–602, doi:10.2475/ajs.303.7.565.
Lucente, C. C., and G. A. Pini (2008), Basin-wide mass-wasting complexes as markers of the Oligo-Miocene foredeep-accretionary wedge evolution in the Northern Apennines, Italy, *Basin Res.*, *20*(1), 49–71, doi:10.1111/j.1365-2117.2007.00344.x.
Luján, M., J. C. Balanyá, and A. Crespo-Blanc (2000), Contractional and extensional tectonics in Flysch and Penibetic units (Gibraltar Arc, SW Spain): New constraints on emplacement mechanisms, *C. R. Acad. Sci., Ser. IIA Earth Planet. Sci.*, *330*(9), 631–637, doi:10.1016/S1251-8050(00)00200-7.
Luján, M., F. Storti, J. C. Balanyá, A. Crespo-Blanc, and F. Rossetti (2003), Role of décollement material with different rheological properties in the structure of the Aljibe thrust imbricate (Flysch Trough, Gibraltar Arc): An analogue modelling approach, *J. Struct. Geol.*, *25*(6), 867–881, doi:10.1016/S0191-8141(02)00087-1.
Macedo, J., and S. Marshak (1999), Controls on the geometry of fold-thrust belt salients, *Geol. Soc. Am. Bull.*, *111*(12), 1808–1822, doi:10.1130/0016-7606(1999)111<1808:COTGOF>2.3.CO;2.
Malavieille, J., and J. F. Ritz (1989), Mylonitic deformation of evaporites in décollements: Examples from the Southern Alps, France, *J. Struct. Geol.*, *11*(5), 583–590, doi:10.1016/0191-8141(89)90089-8.

Mancilla, F. L., G. Booth-Rea, D. Stich, J. V. Pérez-Peña, J. Morales, J. M. Azañón, R. Martin, and F. Giaconia (2015), Slab rupture and delamination under the Betics and Rif constrained from receiver functions, *Tectonophysics*, doi:10.1016/j.tecto.2015.06.028.

Martínez del Olmo, W., and D. Martín (2016), El Neógeno de la Cuenca Guadalquivir-Cádiz (Sur de España), *Rev. Soc. Geol. Esp.*, *29*(1), 35–58.

Martínez-Díaz, J. J. (2002), Stress field variation related to fault interaction in a reverse oblique-slip fault: The Alhama de Murcia fault, Betic Cordillera, Spain, *Tectonophysics*, *356*(4), 291–305, doi:10.1016/S0040-1951(02)00400-6.

Martínez-Martínez, J. M. (2006), Lateral interaction between metamorphic core complexes and less-extended, tilt-block domains: The Alpujarras strike-slip transfer fault zone (Betics, SE Spain), *J. Struct. Geol.*, *28*, 602–620.

Martínez-Martínez, J. M., and J. M. Azañón (1997), Mode of extensional tectonics in the southeastern Betics (SE Spain): Implications for the tectonic evolution of the peri-Alborán orogenic system, *Tectonics*, *16*(2), 205–225, doi:10.1029/97TC00157.

Martínez-Martínez, J. M., J. I. Soto, and J. C. Balanyá (2002), Orthogonal folding of extensional detachments: Structure and origin of the Sierra Nevada elongated dome (Betics, SE Spain), *Tectonics*, *21*(3), 3–1–3–20, doi:10.1029/2001TC001283.

Martín, J. M., J. C. Braga, J. Aguirre, and Á. Puga-Bernabéu (2009), History and evolution of the North-Betic Strait (Prebetic Zone, Betic Cordillera): A narrow, early Tortonian, tidal-dominated, Atlantic–Mediterranean marine passage, *Sediment. Geol.*, *216*(3–4), 80–90, doi:10.1016/j.sedgeo.2009.01.005.

Medialdea, T., R. Vegas, L. Somoza, J. T. Vázquez, A. Maldonado, V. Díaz del Río, A. Maestro, D. Córdoba, and M. C. Fernández-Puga (2004), Structure and evolution of the "Olistostrome" complex of the Gibraltar Arc in the Gulf of Cádiz (eastern Central Atlantic): Evidence from two long seismic cross-sections, *Mar. Geol.*, *209*(1–4), 173–198, doi:10.1016/j.margeo.2004.05.029.

Meijninger, B. M. L., and R. L. M. Vissers (2007), Thrust-related extension in the Prebetic (southern Spain) and closure of the North Betic Strait, *Rev. Soc. Geol. Esp.*, *20*(3–4), 153–171.

Michard, A., D. F. de Lamotte, and A. Chalouan (2005), Comment on "The ultimate arc: Differential displacements, oroclinal bending, and vertical axis rotation in the External Betic-Rif arc" by J. P. Platt et al., *Tectonics*, *24*, TC1005, doi:10.1029/2003TC001603.

Moore, G. F., T. H. Shipley, P. L. Stoffa, D. E. Karig, A. Taira, S. Kuramoto, H. Tokuyama, and K. Suyehiro (1990), Structure of the Nankai Trough accretionary zone from multichannel seismic reflection data, *J. Geophys. Res.*, *95*(B6), 8753–8765, doi:10.1029/JB095iB06p08753.

Morales, J., J. M. Azañón, D. Stich, F. J. Roldán, J. V. Pérez-Peña, R. Martín, J. V. Cantavella, J. B. Martín, F. Mancilla, and A. González-Ramón (2015), The 2012–2013 earthquake swarm in the eastern Guadalquivir Basin (South Spain): A case of heterogeneous faulting due to oroclinal bending, *Gondwana Res.*, *28*(4), 1566–1578, doi:10.1016/j.gr.2014.10.017.

Moresi, L., P. G. Betts, M. S. Miller, and R. A. Cayley (2014), Dynamics of continental accretion, *Nature*, *508*(7495), 245–248, doi:10.1038/nature13033.

Moretti, I., M. Principaud, P. Baby, and J. P. Callot (2010), The role of the evaporite in the Peruvian foreland structural style (North Ucayali), in *Society of Petroleum Engineers - 72nd European Association of Geoscientists and Engineers Conference and Exhibition 2010* - Incorporating SPE EUROPEC 2010, vol. 3, pp. 2078–2082.

Motis, K., and W. Martínez del Olmo (2012), Los cabalgamientos ciegos del Alto Guadalquivir (provincia de Jaén), *Geotemas*, *13*, 1–4.

Murphy, M. A., and P. Copeland (2005), Transtensional deformation in the central Himalaya and its role in accomodating growth of the Himalayan orogen, *Tectonics*, *24*, TC4012, doi:10.1029/2004TC001659.

Nebbad, F. (2001), Le prisme orogenique Prebétique (Sud-Est de l'Espagne), Évolution cinématique et coupes equilibrées, PhD thesis, Orsay, París.

Ogata, K., G. A. Pini, D. Carè, M. Zélic, and F. Dellisanti (2012), Progressive development of block-in-matrix fabric in a shale-dominated shear zone: Insights from the Bobbio Tectonic Window (Northern Apennines, Italy), *Tectonics*, *31*, TC1003, doi:10.1029/2011TC002924.

Ori, G. G., and P. F. Friend (1984), Sedimentary basins formed and carried piggyback on active thrust sheets, *Geology*, *12*(8), 475–478, doi:10.1130/0091-7613(1984)12<475:SBFACP>2.0.CO;2.

Page, B. M. (1963), Gravity tectonics near Passo Della Cisa, Northern Apennines, Italy, *Geol. Soc. Am. Bull.*, *74*(6), 655–671, doi:10.1130/0016-7606(1963)74[655:GTNPDC]2.0.CO;2.

Pedrera, A., C. Marín-Lechado, S. Martos-Rosillo, and F. J. Roldán (2012), Curved fold-and-thrust accretion during the extrusion of a synorogenic viscous allochthonous sheet: The Estepa Range (External Zones, Western Betic Cordillera, Spain), *Tectonics*, *31*, TC4013, doi:10.1029/2012TC003119.

Pedrera, A., A. Ruiz-Constán, C. Marín-Lechado, J. Galindo-Zaldívar, A. González, and J. A. Peláez (2013), Seismic transpressive basement faults and monocline development in a foreland basin (Eastern Guadalquivir, SE Spain), *Tectonics*, *32*, 1571–1586, doi:10.1002/2013TC003397.

Perconig, E. (1960), Sur la constitution géologique de l'Andalousie occidentale, en particulier du bassin du Guadalquivir (Espagne méridionale), Livre en Mémoire du Professeur Paul Fallot, Mémoire Hors de Série, *Bull. Soc. Geol. Fr.*, *229–256*.

Pérez-López, A. (1991), El trías de facies germánica del sector central de la Cordillera Bética, Universidad de Granada, PhD thesis, Departamento de Estratigrafía y Paleontología, Univesidad de Granada, Spain.

Pérez-López, A. (1996), Sequence model for coastal-plain depositional systems of the Upper Triassic (Betic Cordillera, southern Spain), *Sediment. Geol.*, *101*(1–2), 99–117, doi:10.1016/0037-0738(95)00050-X.

Pérez-López, A. (1998), Epicontinental Triassic of the Southern Iberian Continental Margin (Betic Cordillera, Spain), in *Epicontinental Triassic*, edited by G. H. Bachmann and I. Lerche, pp. 1009–1031, Zentralblatt für Geologie und Paläontologie, Stuttgart.

Pérez-López, A., and F. Pérez-Valera (2007), Palaeogeography, facies and nomenclature of the Triassic units in the different domains of the Betic Cordillera (S Spain), *Palaeogeogr. Palaeoclimatol. Palaeoecol.*, *254*(3–4), 606–626, doi:10.1016/j.palaeo.2007.07.012.

Pérez-López, A., and C. Sanz de Galdeano (1994), Tectónica de los materiales triásicos en el sector central de la Zona Subbética (Cordillera Bética), *Rev. Soc. Geol. Esp.*, *7*(1–2), 141–153.

Pérez-López, A., F. Pérez-Valera, and A. E. Götz (2012), Record of epicontinental platform evolution and volcanic activity during a major rifting phase: The Late Triassic Zamoranos Formation (Betic Cordillera, S Spain), *Sediment. Geol.*, *247–248*(0), 39–57, doi:10.1016/j.sedgeo.2011.12.012.

Pérez-Valera, F. (2005), Estratigrafía y tectónica del Triásico Sudibérico en el sector oriental de la Cordillera Bética, Universidad de Granada, PhD thesis, Departamento de Estratigrafía y Paleontología, Univesidad de Granada, Spain.

Pérez-Valera, F., and A. Pérez-López (2007), Stratigraphy and sedimentology of Muschelkalk carbonates of the Southern Iberian Continental Palaeomargin (Siles and Cehegín Formations, Southern Spain), *Facies*, *54*(1), 61–87, doi:10.1007/s10347-007-0125-1.

Pérez-Valera, F., M. Sánchez-Gómez, and A. Pérez-López (2006), Estructura y paleogeografía de los materiales del Triásico en la terminación meridional del Arco de Cazorla (Jaén, Cordillera Bética): Implicaciones tectónicas, *Geogaceta*, *40*, 243–246.

Pérez-Valera, F., M. Sánchez-Gómez, L. A. Pérez-Valera, and A. Pérez-López (2010), Deformación en yesos del Triásico en el sector oriental de la Falla de Socovos (sureste de España), *Geogaceta*, *48*, 211–214.

Pérez-Valera, F., M. Sánchez-Gómez, L. A. Pérez-Valera, and A. Pérez-López (2011a), Kinematics of the northern Betic Cordillera from gypsum fabrics (south Spain): Tectonic implications, *Deformation Mechanism, Rheology and Tectonics*. DRT 2011 Meeting, 98, Oviedo, Spain.

Pérez-Valera, F., M. Sánchez-Gómez, and L. A. Pérez-Valera (2011b), From salt diapis to strike-slip tectonic push-up structures: Outcropping examples from the Triassic evaporites of the Betic Cordillera (south-east Spain), *MAPG-AAPG 2nd International Convention, Conference and Exhibition*, Marrakech.

Pérez-Valera, F., M. Sánchez-Gómez, J. A. Peláez, and L. A. Pérez-Valera (2012), Fallas de edad Pleistoceno superior en el entorno del terremoto de Huesa, Jaén (4.4 mbLg, 31/01/2012): Implicaciones sismotectónicas, *Geogaceta*, *52*, 119–122.

Pérez-Valera, L. A., G. Rosenbaum, M. Sánchez-Gómez, A. Azor, J. M. Fernández-Soler, F. Pérez-Valera, and P. M. Vasconcelos (2013), Age distribution of lamproites along the Socovos Fault (southern Spain) and lithospheric scale tearing, *Lithos*, *180–181*, 252–263.

Peybernès, B., M. J. Fondecave-Wallez, and P. Eichène (2001), L'olistostrome coniacien de Lordat (Pyrénées ariégeoises) et son équivalent latéral de Vicdessos, témoins d'un nouveau bassin d'avant-pays au front nord de la Haute Chaîne Primaire, *Geol. Acta*, *14*(5), 289–306, doi:10.1016/S0985-3111(01)01068-3.

Pini, G. A. (1999), Tectonosomes and Olistostromes in the Argille Scagliose of the Northern Apennines, Italy, *Geol. Soc. Am. Spec. Paper*, *335*, 1–70.

Pini, G. A., K. Ogata, A. Camerlenghi, A. Festa, C. C. Lucente, and G. Codegone (2012), Sedimentary mélanges and fossil mass-transport complexes: A key for better understanding submarine mass movements?, in *Submarine Mass Movements and Their Consequences*, edited by Y. Yamada et al., pp. 585–594, Springer, Netherlands.

Platt, J., S. Allerton, A. Kirker, and E. Platzman (1995), Origin of the western Subbetic arc (South Spain): Palaeomagnetic and structural evidence, *J. Struct. Geol.*, *17*(6), 765–775, doi:10.1016/0191-8141(94)00110-L.

Platt, J. P. (1990), Thrust mechanics in highly overpressured accretionary wedges, *J. Geophys. Res.*, *95*(B6), 9025–9034, doi:10.1029/JB095iB06p09025.

Platt, J. P., and R. L. M. Vissers (1989), Extensional collapse of thickened continental lithosphere: A working hypothesis for the Alboran Sea and Gibraltar arc, *Geology*, *17*(6), 540–543, doi:10.1130/0091-7613(1989)017<0540:ECOTCL>2.3.CO;2.

Platt, J. P., S. Allerton, A. Kirker, C. Mandeville, A. Mayfield, E. S. Platzman, and A. Rimi (2003), The ultimate arc: Differential displacement, oroclinal bending, and vertical axis rotation in the External Betic-Rif arc, *Tectonics*, *22*(3), 1017, doi:10.1029/2001TC001321.

Regard, V., O. Bellier, J. C. Thomas, M. R. Abbassi, J. Mercier, E. Shabanian, K. Feghhi, and S. Soleymani (2004), Accommodation of Arabia-Eurasia convergence in the Zagros-Makran transfer zone, SE Iran: A transition between collision and subduction through a young deforming system, *Tectonics*, *23*, TC4007, doi:10.1029/2003TC001599.

Reiter, K., N. Kukowski, and L. Ratschbacher (2011), The interaction of two indenters in analogue experiments and implications for curved fold-and-thrust belts, *Earth Planet. Sci. Lett.*, *302*(1–2), 132–146, doi:10.1016/j.epsl.2010.12.002.

Riaza, C., and W. Martínez del Olmo (1996), Depositional model of the Guadalquivir-Gulf of Cádiz Tertiary basin, in *Tertiary Basins of Spain: The Stratigraphic Record of Crustal Kinematics*, edited by P. F. Friends and C. J. Dabrio, pp. 330–338, Cambridge Univ. Press, U. K.

Roca, E., P. Anadón, R. Utrilla, and A. Vázquez (1996), Rise, closure and reactivation of the Bicorb–Quesa evaporite diapir, eastern Prebetics, Spain, *J. Geol. Soc. London*, *153*(2), 311–321.

Rodríguez-Fernández, J., and C. Sanz de Galdeano (1992), Onshore Neogene stratigraphy in the North of the Alboran Sea (Betic Internal Zones): Paleogeographic implications, *Geo-Mar. Lett.*, *12*(2–3), 123–128, doi:10.1007/BF02084922.

Rodríguez-Fernández, J., F. J. Roldán, J. M. Azañón, and A. García-Cortés (2013), El colapso gravitacional del frente orogénico alpino en el Dominio Subbético durante el Mioceno medio-superior: El Complejo Extensional Subbético, *Bol. Geol. Min.*, *124*(3), 477–504.

Roldán-García, F. J. (1994), Evolución neógena de la cuenca del Guadalquivir, Universidad de Granada, PhD thesis, Departamento de Estratigrafía y Paleontogogía, Universidad de Granada, Spain.

Roldán-García, F. J., and A. García-Cortés (1988), Implicaciones de materiales triásicos en la Depresión del Guadalquivir (Provincias de Córdoba y Jaén), in *Libro de Resúmenes*, edited by J. A. Vera, pp. 189–192, Granada, Spain.

Roldán-García, F. J., J. Rodríguez-Fernández, and J. M. Azañón (2012), Unidad Olistostrómica, una formación clave para entender la historia neógena de las Zonas Externas de la Cordillera Bética, *Geogaceta*, *52*, 103–106.

Rosell, O., A. Martí, À. Marcuello, J. Ledo, P. Queralt, E. Roca, and J. Campanyà (2011), Deep electrical resistivity structure of the northern Gibraltar Arc (western Mediterranean): Evidence of lithospheric slab break-off, *Terra Nova*, *23*, 179–186, doi:10.1111/j.1365-3121.2011.00996.x.

Rosenbaum, G. (2012), Oroclines of the southern New England orogen, eastern Australia, *Geol. Surv. NSW Episodes*, *35*(1), 187–194.

Rouchy, J. M., E. Groessens, and A. Laumondais (1993), Dislocation of the evaporitic formations under tectonic and dissolution controls: The model of the Dinantian evaporites from Variscan area, northern France and Belgium, *Bull. Soc. Geol. Fr.*, *164*(1), 39–50.

Ruano, P., J. Galindo-Zaldívar, and A. Jabaloy (2004), Recent tectonic structures in a transect of the Central Betic Cordillera, *Pure Appl. Geophys.*, *161*(3), 541–563, doi:10.1007/s00024-003-2462-5.

Ruh, J. B., T. Gerya, and J. P. Burg (2013), High-resolution 3D numerical modeling of thrust wedges: Influence of décollement strength on transfer zones, *Geochem. Geophys. Geosyst.*, *14*, 1131–1155, doi:10.1002/ggge.20085.

Ruiz-Constán, A., D. Stich, J. Galindo-Zaldívar, and J. Morales (2009), Is the northwestern Betic Cordillera mountain front active in the context of the convergent Eurasia–Africa plate boundary?, *Terra Nova*, *21*(5), 352–359, doi:10.1111/j.1365-3121.2009.00886.x.

Ruiz-Constán, A., A. Pedrera, J. Galindo-Zaldívar, J. Pous, J. Arzate, F. J. Roldán-García, C. Marín-Lechado, and F. Anahnah (2012), Constraints on the frontal crustal structure of a continental collision from an integrated geophysical research: The central-western Betic Cordillera (SW Spain), *Geochem. Geophys. Geosyst.*, *13*, Q08012, doi:10.1029/2012GC004153.

Rutter, E. H., R. H. Maddock, S. H. Hall, and S. H. White (1986), Comparative microstructures of natural and experimentally produced clay-bearing fault gouges, *Pure Appl. Geophys.*, *124*(1–2), 3–30, doi:10.1007/BF00875717.

Sample, J. C., and D. M. Fisher (1986), Duplex accretion and underplating in an ancient accretionary complex, Kodiak Islands, Alaska, *Geology*, *14*(2), 160–163, doi:10.1130/0091-7613(1986)14<160:DAAUIA>2.0.CO;2.

Sánchez-Gómez, M., J. A. Peláez, F. J. García-Tortosa, F. Pérez-Valera, and C. Sanz de Galdeano (2014), La serie sísmica de Torreperogil (Jaén, Cuenca del Guadalquivir oriental): Evidencias de deformación tectónica en el área epicentral, *Rev. Soc. Geol. Esp.*, *27*(1), 301–318.

Sans, M. (2003), From thrust tectonics to diapirism. The role of evaporites in the kinematic evolution of the eastern South Pyrenean front, *Geol. Acta*, *1*(3), 239–259.

Sanz de Galdeano, C. (2003), Presencia de estructuras oblicuas en el sector central del Subbético y significado de la falla de Tíscar (Cordillera Bética), *Rev. Soc. Geol. Esp.*, *16*(1–2), 103–110.

Sanz de Galdeano, C., and P. Alfaro (2004), Tectonic significance of the present relief of the Betic Cordillera, *Geomorphology*, *63*(3–4), 175–190, doi:10.1016/j.geomorph.2004.04.002.

Sanz de Galdeano, C., J. Galindo-Zaldívar, A. C. López-Garrido, P. Alfaro, F. Pérez-Valera, A. Pérez-López, and F. J. García-Tortosa (2006), La falla de Tíscar: Su significado en la terminación sudoeste del arco Prebético, *Rev. Soc. Geol. Esp.*, *19*(3–4), 271–280.

Sanz de Galdeano, C., F. J. García-Tortosa, and J. A. Peláez (2013), Estructura del Prebético de Jaén (sector de Bedmar), su relación con el avancel del subbético y con fallas en el basamento, *Rev. Soc. Geol. Esp.*, *26*(1), 55–68.
Seaton, W. J., and T. J. Burbey (2002), Evaluation of two-dimensional resistivity methods in a fractured crystalline-rock terrane, *J. Appl. Geophys.*, *51*(1), 21–41, doi:10.1016/S0926-9851(02)00212-4.
Serrano, I., F. Torcal, and J. B. Martín (2015), High resolution seismic imaging of an active fault in the eastern Guadalquivir Basin (Betic Cordillera, Southern Spain), *Tectonophysics*, *660*, 79–91, doi:10.1016/j.tecto.2015.08.020.
Schlüter, H. U., A. Prexl, C. Gaedicke, H. Roeser, C. Reichert, H. Meyer, and C. von Daniels (2002), The Makran accretionary wedge: Sediment thicknesses and ages and the origin of mud volcanoes, *Mar. Geol.*, *185*(3–4), 219–232, doi:10.1016/S0025-3227(02)00192-5.
Schorn, A., and F. Neubauer (2011), Emplacement of an evaporitic mélange nappe in central Northern Calcareous Alps: Evidence from the Moosegg Klippe (Austria), *Aust. J. Earth Sci.*, *104*(2), 22–46.
Schorn, A., F. Neubauer, and M. Bernroider (2013a), Polyhalite microfabrics in an Alpine evaporite mélange: Hallstatt, Eastern Alps, *J. Struct. Geol.*, *46*, 57–75, doi:10.1016/j.jsg.2012.10.006.
Schorn, A., F. Neubauer, J. Genser, and M. Bernroider (2013b), The Haselgebirge evaporitic mélange in central Northern Calcareous Alps (Austria): Part of the Permian to Lower Triassic rift of the Meliata ocean?, *Tectonophysics*, *583*, 28–48, doi:10.1016/j.tecto.2012.10.016.
Shaw, J., S. T. Johnston, and G. Gutiérrez-Alonso (2016), Orocline formation at the core of Pangea: A structural study of the Cantabrian orocline, NW Iberian Massif, *Lithosphere*, *8*(1), 97, doi:10.1130/L461.1.
Seber, D., M. Barazangi, A. Ibenbrahim, and A. Demnati (1996), Geophysical evidence for lithospheric delamination beneath the Alboran Sea and Rif–Betic mountains, *Nature*, *379*(6568), 785–790, doi:10.1038/379785a0.
Sierro, F. J., J. A. González Delgado, C. Dabrio, J. A. Flores, and J. Civis (1996), Late Neogene depositional sequences in the foreland basin of Guadalquivir (SW Spain), in *Tertiary Basins of Spain: The Stratigraphic Record of Crustal Kinematics*, edited by P. F. Friend and C. J. Dabrio, pp. 339–345, Cambridge Univ. Press, U. K.
Sippl, C., B. Schurr, J. Tympel, S. Angiboust, J. Mechie, X. Yuan, F. M. Schneider, S. V. Sobolev, L. Ratschbacher, and C. Haberland (2013), Deep burial of Asian continental crust beneath the Pamir imaged with local earthquake tomography, *Earth Planet. Sci. Lett.*, *384*, 165–177, doi:10.1016/j.epsl.2013.10.013.
Smit, J., J. P. Burg, A. Dolati, and D. Sokoutis (2010), Effects of mass waste events on thrust wedges: Analogue experiments and application to the Makran accretionary wedge, *Tectonics*, *29*, TC3003, doi:10.1029/2009TC002526.
Sobel, E. R., L. M. Schoenbohm, J. Chen, R. Thiede, D. F. Stockli, M. Sudo, and M. R. Strecker (2011), Late Miocene–Pliocene deceleration of dextral slip between Pamir and Tarim: Implications for Pamir orogenesis, *Earth Planet. Sci. Lett.*, *304*(3–4), 369–378, doi:10.1016/j.epsl.2011.02.012.
Spakman, W., and R. Wortel (2004), A tomographic view on western Mediterranean geodynamics, in *The TRANSMED Atlas. The Mediterranean Region From Crust to Mantle*, edited by P. D. W. Cavazza et al., pp. 31–52, Springer, Berlin, Heidelberg.
Takagi, H. (1998), Fault rocks in the cataclastic–plastic transition zone [in Japanese with English abstract], *Mem. Geol. Soc. Jpn.*, *50*, 59–72.
Talbot, C. J., and V. Pohjola (2009), Subaerial salt extrusions in Iran as analogues of ice sheets, streams and glaciers, *Earth Sci. Rev.*, *97*(1–4), 155–183, doi:10.1016/j.earscirev.2009.09.004.
Trudgill, B. D. (2011), Evolution of salt structures in the northern Paradox Basin: Controls on evaporite deposition, salt wall growth and supra-salt stratigraphic architecture, *Basin Res.*, *23*(2), 208–238, doi:10.1111/j.1365-2117.2010.00478.x.
Trusheim, F. (1960), Mechanism of salt migration in northern Germany, *AAPG Bull.*, *44*(9), 1519–1540.
Vannucchi, P., and G. Bettelli (2010), Myths and recent progress regarding the Argille Scagliose, Northern Apennines, Italy, *Int. Geol. Rev.*, *52*(10–12), 1106–1137, doi:10.1080/00206810903529620.
Vannucchi, P., A. Maltman, G. Bettelli, and B. Clennell (2003), On the nature of scaly fabric and scaly clay, *J. Struct. Geol.*, *25*(5), 673–688, doi:10.1016/S0191-8141(02)00066-4.
Vera, J. A. (2001), Evolution of the South Iberian continental margin, *Mémoires du Muséum national d'histoire naturelle*, *186*, 109–143.
Vera, J. A., and J. M. Molina (1999), The Capas Rojas Formation: Characterization and genesis, *Estud. Geol.*, *55*(1–2), 45–66.
Vitale, S., M. N. Zaghloul, B. El Ouaragli, F. D. A. Tramparulo, and S. Ciarcia (2015), Polyphase deformation of the Dorsale Calcaire Complex and the Maghrebian Flysch Basin Units in the Jebha area (Central Rif, Morocco): New insights into the Miocene tectonic evolution of the Central Rif belt, *J. Geodyn.*, *90*, 14–31, doi:10.1016/j.jog.2015.07.002.
Wenkert, D. D. (1979), The flow of salt glaciers, *Geophys. Res. Lett.*, *6*(6), 523–526, doi:10.1029/GL006i006p00523.
Westbrook, G. K., J. W. Ladd, P. Buhl, N. Bangs, and G. J. Tiley (1988), Cross section of an accretionary wedge: Barbados Ridge complex, *Geology*, *16*(7), 631–635, doi:10.1130/0091-7613(1988)016<0631:CSOAAW>2.3.CO;2.
Wu, S., A. W. Bally, and C. Cramez (1990), Allochthonous salt, structure and stratigraphy of the north-eastern Gulf of Mexico. Part II: Structure, *Mar. Pet. Geol.*, *7*(4), 334–370, doi:10.1016/0264-8172(90)90014-8.
Zweigel, P. (1998), Arcuate accretionary wedge formation at convex plate margin corners: Results of sandbox analogue experiments, *J. Struct. Geol.*, *20*(12), 1597–1609, doi:10.1016/S0191-8141(98)00052-2.